

Geometric realizations of ν -associahedra via brick polyhedra

Master Thesis

to achieve the university degree of
Master of Science

submitted to Graz University of Technology

By

Matthias MÜLLER, BSc.

Institute of Geometry

Supervisor: Priv.-Doz. Mag. Dr.rer.nat. Mat. Cesar Ceballos

Graz, 12. Juli 2024



This Master Thesis is supervised
by Priv.-Doz. Mag. Dr.rer.nat. Mat. Cesar Ceballos

**He who understands geometry
is able to understand everything in this world. [Sch]**

Galileo Galilei (1564 - 1642)

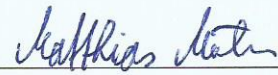
Acknowledgement

My main thanks go to Priv.-Doz. Mag. Dr.rer.nat Mat. Cesar Ceballos for the motivating conversations, competent advice and friendly support with care of this master's thesis. Owing to your fascinating lecture and introduction of associahedra, I decided to make "Brick Polyhedra" my work.

Declaration of originality

I declare that I have authored this thesis independently, that I have not used other than the declared sources / resources, and that I have explicitly marked all material which has been quoted either literally or by content from the used sources.

Graz, 12. Juli 2024



Matthias Müller, BSc.

Abstract

This master's thesis gives a new geometric realization, as the edge graph of a polytopal complex, of the rotation lattice of ν -trees using a projection of a brick polyhedron. Motivated by the fact that generalized associahedra for cluster algebras can be realized as brick polytopes, this concept has been generalized for all subword complexes, known as the brick polyhedron, which is in the center of this thesis. After introducing the allowed tools, we give a projection of a brick polyhedron to obtain a new realization of the ν -associahedron.

Table of Content

Acknowledgement	III
Abstract	V
1 Preliminaries	1
1.1 A little thought experiment	1
1.2 Coxeter groups	2
2 Brick polyhedra	7
2.1 Brick polytopes of sorting networks	7
2.2 Brick polytopes of spherical subword complexes	13
2.3 Brick polyhedra	16
3 Application	20
3.1 The ν -Tamari lattice	20
3.2 The ν -Tamari complex and the ν -subword complex	22
3.3 The ν -associahedron	23
3.3.1 A canonical realization of the alt ν -associahedron	25
3.4 A geometric realization via brick polyhedra	27
3.4.1 Faces of brick polyhedra	27
3.4.1.1 The minimal element of a face	29
3.4.1.2 Characterization of the vertices in a face F	29
3.4.1.3 Proof of Theorem 3.23	31
3.4.2 Some faces of ν -brick polyhedra	32
3.4.3 Bounded faces of ν -brick polyhedra	36
3.4.3.1 The spherical and root independent property	36
3.4.3.2 Unique representation of bounded faces	39
3.4.4 The poset of bounded faces of ν -brick polyhedra	40
3.5 A projection of brick polyhedra	40
3.5.1 The maximal polytopal part	41
3.5.2 A projection in a special case	42
3.5.3 A projection in the general case	47
Bibliography	52

1 Preliminaries

The word “geometry” comes from ancient Greek, consisting of “geo” (earth) and “metro” (measure). Therefore, philosophically geometry can be seen as “measuring the earth”. We will always consider a finite dimensional vector spaces V over a field k , which can be described/characterized indirectly by defining its dual $V^* := \{\lambda : V \rightarrow k \mid \lambda \text{ is } k\text{-linear}\}$. Since $V \cong (V^*)^*$, we can recover V from the space of linear functions on V . This work considers finite Coxeter groups of type A as thinking about “geo” (earth) and a counting measure in respect of “metron” (measure). In Chapter 3 we will see what we are measuring out. For the motivation of considering brick polytopes, we will give a little thought experiment for obtaining the permutahedron of order four, which can be realized geometrically using brick polytopes. In the second part of this chapter we give a brief introduction of Coxeter groups.

1.1 A little thought experiment

In geometry, the truncated octahedron is a very interesting object. As it is often motivated by the Catalan numbers, we will start with a little thought experiment, where the truncated octahedron appears. Moreover, the truncated octahedron is also known as the permutahedron of order four, which is a three-dimensional polytope.

In 1927, Edwin Hubble presented the observation that the universe is expanding. So, it will be intuitive to think about some boundary of the whole space. Let us model the space by a three-dimensional expanding ball. In the next step, we consider a spaceship in our ball. If the spaceship flies with an infinite energy source, we can consider the case reaching the boundary of the space. As our ball is the whole space we come to the conclusion that if we cross the boundary the spaceship will appear on the other side of the ball. Regarding that this sounds a bit unrealistic in physics, we consider this as an entry of our spaceship in an exact copy of our ball. Doing this for all directions, we come to the conclusion that our ball could not fill the whole space without some tiling space. From this, our assumption of the boundary in the form of a ball does not make sense anymore. But we are very interested in space filling polyhedra. The next idea will be to replace the ball by a cube. This polyhedron fills the whole space and this assumption sounds very comfortable. Now in each vertex of the cube eight copies of our space contact and this does not make much sense. For this, we can consider the truncated octahedron. It fills the space and in each vertex we observe that exactly three edges of four polytopes touch. Technically speaking, this gives us a better understanding, why we are living in a three-dimensional space.

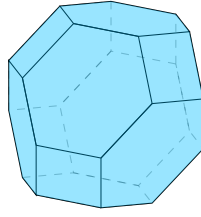


Figure 1.1: Truncated octahedron with f-vector $(24,36,14)$.

We also know the truncated octahedron by the Kelvin problem, posed by Lord Kelvin in 1887, which is given by finding an arrangement of polyhedra of equal volume, such that the total surface area of the surfaces between them is as small as possible. From this conclusion, we are very interested in studying the truncated octahedron and get a better understanding of its geometry.

General Sidemark: If we contract some faces and edges of the truncated octahedron, we get some realization of the associadron (special case of the secondary polytope). For studying the combinatorics of these polytopes, we identify polytopes with the same face lattice. To remember, this is the partially ordered set (poset) whose elements are the faces of the polytope, including the polytope itself, its faces, edges vertices and the “empty” face (ordered in levels with this order) and connected by an edge, if there is a contact in the polytope. We will identify two polytopes, if they have the same face lattice, and ask, if there is a polytope realizing a given face lattice. In analogy to this, we will see that the brick polytope realizes subgraphs of the flip graph.

1.2 Coxeter groups

We give a short introduction to finite Coxeter groups. Our Coxeter systems are representing symmetry groups, which are generated by reflections. Their elements can be classified by their reduced expressions. We will see two key properties about them. We concentrate on Coxeter groups of type A. The definitions are taken from [Hum90].

A Coxeter system is defined as a pair (W, S) consisting of a finite set of generators $S \subset W$ and a group W , called Coxeter group¹, subject to relations of the form $(ss')^{m(s,s')} = e$, where $m(s, s) = 1$, $m(s, s') = m(s', s) \geq 2$, for two distinct elements $s, s' \in S$ and e being the identity. In this setup we are going to allow the case $m(s, s') = \infty$, if s and s' are unrelated. The cardinality of S is denoted by $|S|$, called the rank of the Coxeter system (W, S) . Therefore, we use the following notation for a Coxeter group: $W = \langle S \mid (st)^{m(s,t)} = e \rangle$. We can represent a Coxeter System (W, S) by a Coxeter graph having a vertex for each generator $s \in S$ and an edge (s, s') if $m(s, s') \geq 3$. The edges are labeled with the number $m(s, s')$ if $m(s, s') > 3$, edges without number correspond to order $m(s, s') = 3$ and we do not draw the edges for $m(s, s') = 2$ since this means that the elements commute, i.e. $ss' = s's$ for $s, s' \in S$, several examples are shown in Figure 1.2.

Example 1.1: Coxeter group of type A_n

The Coxeter group of type A_n is the group generated by $S = \{s_1, \dots, s_n\}$ satisfying $s_i^2 = e$ for $i = 1, \dots, n$. $(s_i s_{i+1})^3 = e$ for $i = 1, \dots, n-1$ and $s_i s_j = s_j s_i = e$ for $|i - j| > 1$. The Coxeter group of type A_2 describes the symmetry group of an equilateral triangle. A_3 describes the symmetry

¹ W is acting on an Euclidean vector space $V \cong \mathbb{R}^n$, where $n = |S|$.

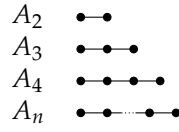


Figure 1.2: Coxeter graphs of type A.

group of a tetrahedron, which is exactly the same as the symmetry group \mathcal{S}_4 of permutations of four elements. The Coxeter graph of A_4 will consist of four vertices, connected by three edges and describes the symmetry group of a 4-dimensional simplex. In general, A_n is the symmetry group of an n -simplex. It can be shown that the Coxeter group A_n is isomorphic to the symmetric group \mathcal{S}_{n+1} of permutations of $n + 1$ elements. In symbols: $W_{A_n} \cong \mathcal{S}_{n+1}$.

Each generator has order 2 in W , every $s \in S$ satisfies $m(s, s) = 2$, and each $w \neq e$ can be written as $w = s_1 \cdots s_k$ for some $s_i \in S$, which are not necessarily distinct. We call the smallest possible k the length of w , and denote it by $\ell(w)$. Any expression of w as a product of k elements of S is called a reduced expression of w . In particular $w = s_1 \cdots s_k$ is reduced if $\ell(w) = k$. In general, we distinguish between the word (s_1, \dots, s_k) and the product $s_1 \cdots s_k$. Reduced expressions in W are fundamental in the study of Coxeter groups. They satisfy two useful properties called the Strong Exchange Property and the Deletion Property [Hum90].

Theorem 1.2: Strong Exchange Property [Hum90]

Let $w = s_1 \cdots s_k$ be a not necessarily reduced word in S and $t \in S$ such that $\ell(wt) < \ell(w)$. Then there exists an index i such that $wt = s_1 \cdots \hat{s}_i \cdots s_k$. This notation means that the i -th component is omitted.

The proof of this Theorem also works for the following statement: If $t \in S$ satisfies $\ell(tw) < \ell(w)$ then $tw = s_1 \cdots \hat{s}_i \cdots s_k$. If the expression for w is reduced, then the index i , which is omitted is unique.

Theorem 1.3: Deletion Property [Hum90]

Let $w = s_1 \cdots s_k$ be a word in S such that $\ell(w) < k$. Then there exist indices $i < j$ for which $w = s_1 \cdots \hat{s}_i \cdots \hat{s}_j \cdots s_k$ holds.

Furthermore, finite Coxeter groups have a nice representation as a group generated by reflections in a vector space V . We will denote by s_v for $v \in V \setminus \{0\}$ the reflection interchanging v and $-v$, which is fixing the orthogonal hyperplane $v^\perp = \{w \in V \mid \langle v, w \rangle = 0\}$ pointwise. Recall that W is acting on a finite vector space V , and one can find a basis $\{\alpha_1, \dots, \alpha_n\}$ of $V \cong \mathbb{R}^n$, called simple roots, with inner form² $\langle \cdot, \cdot \rangle$ and $|S| = n$, such that $s_i = s_{\alpha_i}$. In other words, W is the group generated by reflections along hyperplanes orthogonal to the simple roots $\alpha_1, \dots, \alpha_n$.

Define the root system $\Phi := \{w\alpha_i \mid w \in W, 1 \leq i \leq n\}$ as the set obtained by letting all group elements of W act on our α_i 's. We say that a root $\beta \in \Phi$ is positive, if it can be written as a linear combination of simple roots $\beta = c_1\alpha_1 + \cdots + c_n\alpha_n$, such that all coefficients are non-negative $c_i \geq 0 \forall i \in [n]$, and a negative root if all coefficients are non-positive $c_i \leq 0 \forall i \in [n]$. The set

2) This needs some details about the geometric representation of W . We refer to [Hum90] for more details.

of positive roots (resp. negative roots) is denoted by Φ^+ (resp. Φ^-). A useful theorem from reflection groups [Hum90] tells us that the set of roots can be written as disjoint union of positive and negative roots $\Phi = \Phi^+ \sqcup \Phi^-$.

Remark 1.4

As a consequence, there exists a hyperplane H , known as the root hyperplane, that separates the positive roots Φ^+ and negative roots Φ^- . There is a normal vector to this hyperplane, denoted as η , such that the linear functional $\eta : V \rightarrow \mathbb{R}$, $\eta(x) := \langle \eta, x \rangle$ is positive for positive roots and negative for negative roots, meaning $\langle \alpha, \eta \rangle > 0$ for $\alpha \in \Phi^+$ and $\langle \alpha, \eta \rangle < 0$ for $\alpha \in \Phi^-$. Moreover, $\langle \eta, \alpha \rangle \neq 0$ for all $\alpha \in \Phi$.

The set of reflections in W is defined by $\mathcal{R} := \{ws w^{-1} \mid w \in W, s \in S\}$, and corresponds to geometric reflections along positive roots $\{s_\beta \mid \beta \in \Phi^+\}$. In particular, we associate to each simple reflection $s \in \mathcal{R}$ a simple root $\alpha_s \in V$, and denote the set of simple roots by $\Lambda = \{\alpha_s \mid s \in S\}$. This is a subset of the set of reflections $\mathcal{R} = \{s_\beta \mid \beta \in \Phi^+\}$.

Example 1.5: Root systems of type A_n

Let $V = \mathbb{R}^{n+1}$ with standard inner product and $\{e_1, \dots, e_{n+1}\}$ the basis of canonical unit vectors. Then $\Phi^+ = \{(e_i - e_j) \mid 1 \leq i < j \leq n+1\}$ and $\Phi^- = \{-(e_i - e_j) \mid 1 \leq i < j \leq n+1\}$. The simple roots are $\alpha_i = e_i - e_{i+1}$ and $s_i = s_{\alpha_i}$ for $1 \leq i \leq n$. The generating system is given by $S = \{s_i \mid 1 \leq i \leq n\}$.

Example 1.6: Root system of type A_2

If $n = 2$ we obtain $\Phi^+ = \{e_1 - e_2, e_1 - e_3, e_2 - e_3\}$, $\Phi^- = \{e_2 - e_1, e_3 - e_1, e_3 - e_2\}$. Simple roots $\alpha_1 = e_1 - e_2$, $\alpha_2 = e_2 - e_3$ and $S = \{s_1, s_2\}$, shown in Figure 1.3.

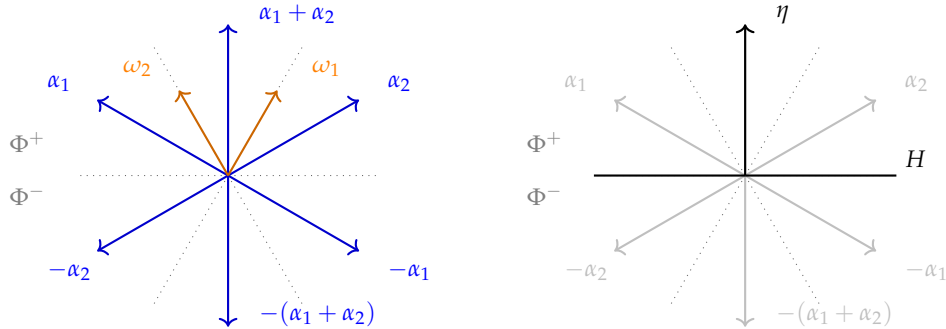


Figure 1.3: Left: Root system of type A_2 Right: Root hyperplane H and Highest root η .

The fundamental weights $\omega_1, \dots, \omega_n$ are defined such that $\langle \alpha_s, \omega_t \rangle = \delta_{s,t} \frac{\langle \alpha_s, \alpha_s \rangle}{2}$. Using the Cartan matrix $C = (c_{i,j})_{i,j \in S}$, with $c_{i,j} = 2 \frac{\langle \alpha_i, \alpha_j \rangle}{\langle \alpha_i, \alpha_i \rangle}$, that gives the nice connection $\underline{\alpha} = C \underline{\omega}$ ³, where $\underline{\alpha}$ and $\underline{\omega}$ are the vectors of simple roots and fundamental weights. The set of fundamental weights is denoted by $\nabla = \{\omega_s \mid s \in S\} \subseteq V$. By the previous discussion, the fundamental weights satisfy $\alpha_s = \sum_{t \in S} c_{ts} \omega_t$ and $s(\omega_t) = \omega_t - \delta_{s=t} \alpha_s$ for $s, t \in S$. Geometrically, the fundamental weights are the directions of the rays spanning the fundamental chamber.

³ This comes from the geometric representation by mapping $W \rightarrow GL(V)$, $s_i \mapsto \sigma_i$ with $\sigma_i(v) := v - 2\langle v, \alpha_i \rangle \alpha_i$

Example 1.7: Fundamental weights of type A_n

The Cartan matrix $C = (c_{ij})_{i,j}$ of the root system A_n is given by

$$c_{ij} = \begin{cases} 2, & \text{if } i = j \\ -1, & \text{if } |i - j| = 1 \\ 0, & \text{otherwise} \end{cases}$$

and therefore invertible. By [LL19] the inverse is given by $(C^{-1})_{i,j} = \min\{i, j\} - \frac{ij}{n+1}$. Therefore, the fundamental weights are given by $\underline{\omega} = C^{-1}\underline{\alpha}$. The i -th fundamental weight is given by $\omega_i = (\underline{\omega})_i = (C^{-1}\underline{\alpha})_i = \sum_j (\min\{i, j\} - \frac{ij}{n+1})\alpha_j = \sum_j \min\{i, j\}\alpha_j - \sum_j \frac{ij}{n+1}\alpha_j$ for $1 \leq i \leq n$.

Example 1.8: Fundamental weights of type A_2

As an example, let us consider a root system of type A_2 . For the corresponding Cartan matrix $C_{A_2} = \begin{pmatrix} 2 & -1 \\ -1 & 2 \end{pmatrix}$ and $C_{A_2}^{-1} = \frac{1}{3} \begin{pmatrix} 2 & 1 \\ 1 & 2 \end{pmatrix}$ we have $\underline{\alpha} = C_{A_2}\underline{\omega}$. We use the notation $10_\Delta = 1\alpha_1 + 0\alpha_2$ and $\overline{10}_\Delta = -1\alpha_1 - 0\alpha_2$. We have $S = \{s_1, s_2\}$, simple and positive roots $\Delta \subset \Phi^+$ given by $\{10_\Delta, 01_\Delta\} \subset \{10_\Delta, 01_\Delta, 11_\Delta\}$ and $s_1(10_\Delta) = \overline{10}_\Delta$, $s_1(01_\Delta) = 11_\Delta$, $s_2(10_\Delta) = 12_\Delta$, $s_2(01_\Delta) = \overline{01}_\Delta$. So we get $\nabla = \{\omega_1 = \frac{1}{3}(21_\Delta), \omega_2 = \frac{1}{3}(12_\Delta)\}$. To practice notation, we show this for α_1 : $a_{11}\omega_1 + a_{21}\omega_2 = 2(\frac{1}{3}(21_\Delta)) + (-1)(\frac{1}{3}(12_\Delta)) = \frac{2}{3}(2\alpha_1 + \alpha_2) - \frac{1}{3}(\alpha_1 + 2\alpha_2) = \alpha_1$.

A connection between positive (resp. negative) roots and the length of a word is given by the following theorem.

Theorem 1.9: [Hum90]

Let $w \in W$ and $s \in S$. If $\ell(ws) < \ell(w)$ then $w(\alpha_s)$ is a negative root. Analogously, if $\ell(ws) > \ell(w)$ then $w(\alpha_s)$ is a positive root.

Example 1.10

Consider a root system of type A_2 . Let $S = \{s_1, s_2\}$ be the generating system and $\alpha_1 = \alpha_{s_1}$, $\alpha_2 = \alpha_{s_2}$ as in Figure 1.3. For $w = s_1s_2$, we obtain $s_1s_2(\alpha_1) = \alpha_2$ and $s_1s_2(\alpha_2) = -(\alpha_1 + \alpha_2)$. Since $\ell(s_1s_2s_1) > \ell(s_1s_2)$, $w(\alpha_1) = \alpha_2$ this is a positive root by Theorem 1.9. Analogously $\ell(s_1s_2s_2) = \ell(s_1) < \ell(s_1s_2)$ implies $w(\alpha_2) = -(\alpha_1 + \alpha_2)$ is a negative root.

We use \leq_B for the Bruhat order on W , which is the partial order defined by the cover relation $w \prec_B rw$ for $w \in W$ and $r \in \mathcal{R}$ with $\ell(rw) = \ell(w) + 1$. A Bruhat interval $[x, y]$ is defined for $x \leq_B y$, by $[x, y] = \{z \in W \mid x \leq z \leq y\}$. Another, well known partial order in W is the right weak order, which differs from the Bruhat order as follows:

- Right weak order: $x \prec_R y \Leftrightarrow s \in S : xs = y$ and $\ell(y) = \ell(x) + 1$
- Bruhat order: $x \prec_B y \Leftrightarrow r \in \mathcal{R} : rx = y$ and $\ell(y) = \ell(x) + 1$

An equivalent definition of right weak order is given by the inversion set $\text{Inv}(w) := \{s_1 \dots s_{k-1}(\alpha_{s_k}) \mid 1 \leq k \leq l\}$ of a reduced element $w = (s_1, \dots, s_l) \in W$, $s_i \in S$. An element x is smaller in right weak order than an element y , if and only if the inversion set of x is contained in the inversion set of y [JS23]. In symbols: $x \leq_R y \Leftrightarrow \text{Inv}(x) \subseteq \text{Inv}(y)$. By definition, right weak order implies Bruhat order.

A concept of great interest for our work is the Demazure product of a word $Q = (s_1, \dots, s_n)$. By [KM04, Lemma 3.4 (1)] the Demazure product of Q can be defined as the unique maximal element in Bruhat order that is a subword of Q

$$\text{Dem}(Q) = \max_{\leq_B} \{ \prod Q_X \mid X \subseteq \{1, \dots, n\} \},$$

where $\prod Q_X$ denotes the product of elements with indices in X . The maximum can easily be calculated by a greedy algorithm using Theorem 1.9. Note that the Demazure product induces a monoid structure on any Coxeter group. By Knutson and Miller [KM04], the Demazure product of a word is essential to determine whether a subword complex is a topological sphere or ball. We will discuss more about this, when we introduce subword complexes in Chapter 3.

2 Brick polyhedra

This chapter starts with the brick polytope of a sorting network and presents some generalization to the brick polytope for spherical subword complexes. The generalization to all subword complexes are called brick polyhedra, which are the heart of our thesis. They will allow us to consider any path ν in our geometric realization of ν -associahedra in Chapter 3.

2.1 Brick polytopes of sorting networks

Before generalizing the brick polytope to finite Coxeter groups, we first study the brick polytope of a sorting network. This part is mainly based on [PS12]. We follow the underlying idea to construct polytopes from combinatorics and explain combinatorics with geometry. We are studying the brick polytope of a network \mathcal{N} . The permutahedron will show up as the brick polytope of the duplicated network. Remark that the permutahedron can be manipulated to obtain some realization of the associahedron. For a detailed construction we refer to [Hoh12], [HL07]. This will be in close connection to the brick polytope. For well chosen networks, the brick polytope coincides with the associahedron of Hohlweg and Lange, shown in [PS12], which gives us a new point of view of their associahedron.

We give a short reminder about the usual setup for a sorting network \mathcal{N} . The network \mathcal{N} is a set of n horizontal lines (levels, labelled from top to bottom) and m vertical segments (commutators, labelled from left to right) joining two levels, where the commutators have pairwise distinct endpoints. The generated bounded cells are called bricks¹. For an example, see Figure 3.23. A pseudoline is a abscissa monotone path on \mathcal{N} which starts at some level k and ends at level $n - k + 1$. We say a commutator is a contact between two pseudolines, if its endpoints are contained in respectively one of them. The set of commutators will be very useful. If a commutator is contained in two pseudolines, it is called a crossing between these pseudolines. A pseudoline arrangement is a set of n pseudolines supported by \mathcal{N} such that any two of them have precisely one crossing, maybe some contacts and no other intersection. Since we define a pseudoline arrangement by having exactly one crossing and our network \mathcal{N} is fixed (and so the commutators) it is completely determined by its $\binom{n}{2}$ crossings or especially by its $m - \binom{n}{2}$ contacts. Such a network is also said to be reduced, if we consider more general networks. \mathcal{N} is called sorting if it supports some pseudoline arrangement. This gives the intuitive sense of sorting, since if we run through the network the order of pseudolines changes.

¹) We are following [PS12] and do not count the first brick, which is only bounded by the right side. In the following part we will note that we later count it. This will not make any differences for our observations.

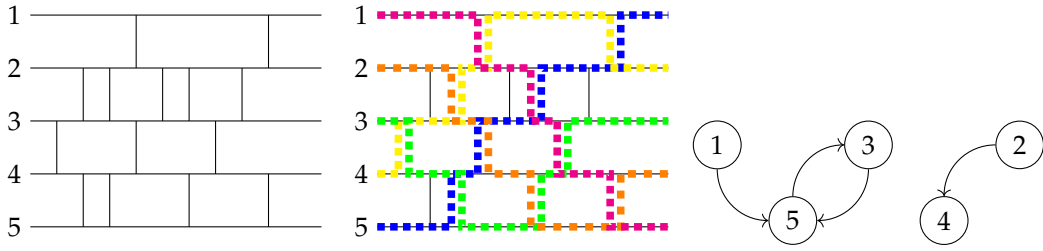


Figure 2.1: Left: sorting network \mathcal{N} with $n = 5$ and $m = 14$, Middle: pseudoline arrangement $\Lambda \in \text{Arr}(\mathcal{N})$, Right: contact graph $\Lambda^\#$.

The set of all pseudoline arrangements supported by \mathcal{N} is denoted by $\text{Arr}(\mathcal{N})$. By this setup, we can transform a pseudoline arrangement supported by \mathcal{N} into another one by exchanging the position of a contact and a crossing of the same two pseudolines, which is called a flip operation. We call the pseudoline arrangement, where any of its contacts is located to the right (resp. left) of its corresponding cross (if any) the greedy (resp. anti-greedy) pseudoline arrangement.

For a given pseudoline arrangement $\Lambda \in \text{Arr}(\mathcal{N})$, the contact graph $\Lambda^\#$ is the directed multigraph with a node for each pseudoline and an arc (i, j) for each contact of Λ oriented from the node for the pseudoline i passing above the contact to the node corresponding to the pseudoline j passing below it. If the contact graph $\Lambda^\#$ is connected (resp. disconnected) the sorting network Λ is called irreducible (resp. reducible). An example for a disconnected contact graph is illustrated in Figure 3.23. Other examples are shown in Figure 2.6.

Now we can define the flip graph $G(\mathcal{N}) = (V(G), E(G))$ with $V(G)$ as the set of pseudoline arrangements supported by \mathcal{N} and $E(G)$ as the set of possible flips between them. An example is shown in Figure 2.2. By Pilaud and Pocchiola [PS12, Theorem 2.1], the flip graph $G(\mathcal{N})$ is $(m - \binom{n}{2})$ -regular and connected.

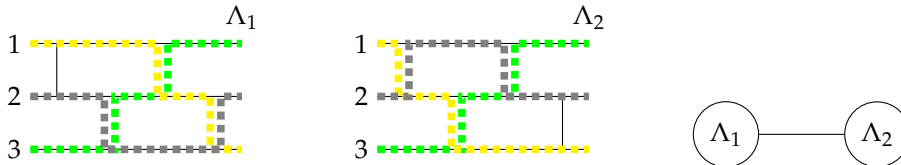


Figure 2.2: Left/Middle: Two pseudoline arrangements Λ_1 and Λ_2 supported by the sorting network \mathcal{N} , related by a flip between the pseudolines 1 and 2. The right (resp. left) pseudoline arrangement is the greedy (resp. antigreedy) pseudoline arrangement. Right: Flip graph $G(\mathcal{N}) = (V(G), E(G))$.

We define the brick polytope of a sorting network as follows:

Definition 2.1: Brick polytope of a sorting network [PS12]

Let \mathcal{N} be a sorting network with n levels. The brick vector of a pseudoline arrangement Λ supported by \mathcal{N} is the vector $b(\Lambda) \in \mathbb{R}^n$ whose i -th coordinate is the number of bricks of \mathcal{N} located below the i -th pseudoline of Λ . The brick polytope $\Omega(\mathcal{N}) \subset \mathbb{R}^n$ of the sorting network \mathcal{N} is the convex hull of the brick vectors $b(\Lambda)$ associated to the pseudoline arrangements Λ supported by \mathcal{N} :

$$\Omega(\mathcal{N}) := \text{conv}\{b(\Lambda) \mid \Lambda \in \text{Arr}(\mathcal{N})\} \subset \mathbb{R}^n$$

The next observation gives us that the brick polytope is not of full dimension. The depth of a brick of \mathcal{N} is defined as the number of levels above it and we denote by $\mathcal{D}(\mathcal{N})$ the sum of the depths of all bricks. By definition of pseudoline arrangements, the number of pseudolines above each brick is equal to its depth. Therefore, the brick polytope is contained in the hyperplane defined by the equation $\sum_{i=1}^n x_i = \mathcal{D}(\mathcal{N})$ and has at most dimension $n - 1$. An interesting example is the “Duplicated Sorting Networks”.

Example 2.2: Duplicated Sorting Network [PS12]

Let \mathcal{N} be a reduced network with n levels and $\binom{n}{2}$ commutators. The duplicated sorting network of \mathcal{N} is defined as the network obtained by duplicating the commutators of \mathcal{N} . In this construction we disallow a crossing between the original commutator and its added twin.

We are going to compute the brick polytope of the duplicated sorting network \mathcal{N} shown in Figure 2.3 and use the notation $(2, 3, 5)$ for the sorting network with commutators 2, 3, 5 as contacts. For the sorting network \mathcal{N} we obtain $2^3 = 8$ possible pseudoline arrangements: $\Lambda_1 = (1, 3, 5)$, $\Lambda_2 = (2, 3, 5)$, $\Lambda_3 = (2, 4, 5)$, $\Lambda_4 = (2, 4, 6)$, $\Lambda_5 = (1, 4, 6)$, $\Lambda_6 = (1, 3, 6)$, $\Lambda_7 = (2, 3, 6)$, $\Lambda_8 = (1, 4, 5)$, illustrated in Figure 2.4. The flip graph is given by a cube, shown in Figure 2.5. Note, this concept can be used to construct a d -dimensional cube, which can be constructed by drawing two $(d - 1)$ -dimensional cubes and connecting each vertex from one cube to its twin in the other cube.

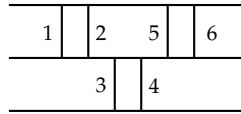


Figure 2.3: Duplicated sorting network \mathcal{N} .

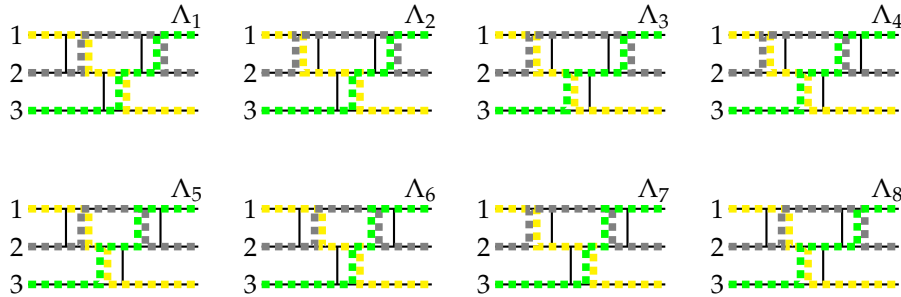


Figure 2.4: Pseudoline arrangements supported by \mathcal{N} from Figure 2.3.

By counting the bricks below each pseudoline, we obtain the following brick vectors:

$$\begin{aligned} b(\Lambda_1) &= (2, 3, 0)^\top & b(\Lambda_2) &= (1, 4, 0)^\top & b(\Lambda_3) &= (0, 4, 1)^\top & b(\Lambda_4) &= (0, 3, 2)^\top \\ b(\Lambda_5) &= (1, 2, 2)^\top & b(\Lambda_6) &= (2, 2, 1)^\top & b(\Lambda_7) &= (1, 3, 1)^\top & b(\Lambda_8) &= (1, 3, 1)^\top \end{aligned}$$

Note, all brick vectors are in the plane $x_1 + x_2 + x_3 = 5$. Therefore, the brick polytope is two dimensional, shown in Figure 2.7.

In Figure 2.6 we observe that the contact graph $\Lambda_6^\#$ is acyclic and $\Lambda_7^\#$ is cyclic. If we compare this with the brick polytope shown in Figure 2.7 we observe that $b(\Lambda_6)$ is on the boundary, whereas $b(\Lambda_7)$ is not.

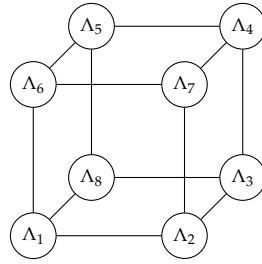


Figure 2.5: Flip graph for the sorting network \mathcal{N} in Figure 2.3.



Figure 2.6: Two contact graphs for the sorting network \mathcal{N} in Figure 2.3.

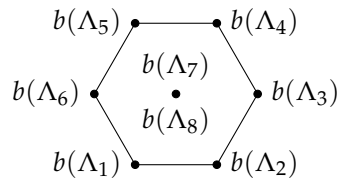


Figure 2.7: Brick polytope obtained by the sorting network in Figure 2.3

Observe two questions: Firstly: What is the exact dimension of the brick polytope? Secondly: Which vertices are vertices of the brick polytope? It is shown that we have the following general statements:

- The brick polytope $\Omega(\mathcal{N})$ satisfies at each brick vector $b(\Lambda)$:
 $\text{cone}\{b(\Lambda') - b(\Lambda) \mid \Lambda' \in \text{Arr}(\mathcal{N})\} = \text{cone}\{e_j - e_i \mid (i, j) \in \Lambda^\#\}. \text{ [PS12, Theorem 3.13]}$
- The brick polytope of an irreducible sorting network with n levels has dimension $n - 1$. The dimension of a brick polytope with n levels and p irreducible components has dimension $n - p$. [PS12, Corollary 3.14]
- The brick vector $b(\Lambda)$, $\Lambda \in \text{Arr}(\mathcal{N})$ is a vertex of $\Omega(\mathcal{N})$, if and only if the corresponding contact graph $\Lambda^\#$ is acyclic. [PS12, Corollary 3.15]

Example 2.3: Permutahedron of order three and four

The brick polytope in Figure 2.2 is isomorphic to the permutahedron of order three. Analogously to Example 2.2, the brick polytope for the duplicated sorting network shown in Figure 2.8 (Left) is isomorphic to the permutahedron of order four in Figure 2.8 (Right).



Figure 2.8: Left: Duplicated sorting network, Right: Corresponding brick polytope isomorphic to permutahedron of order four.

We define the simplicial complex $\Delta(\mathcal{N})$ of all sets of commutators of \mathcal{N} contained in the set of contacts of a pseudoline arrangement supported by \mathcal{N} . This means a set of commutators \mathcal{I} of \mathcal{N} is a face of $\Delta(\mathcal{N})$ if and only if the network $\mathcal{N} \setminus \mathcal{I}$ is still sorting. This complex is pure of dimension $m - \binom{n}{2} - 1$. This motivates Question 2.4.

Question 2.4

Is $\Delta(\mathcal{N})$ the boundary complex of a $m - \binom{n}{2}$ - dimensional simplicial polytope?

The brick polytope was introduced by [PS12] as an attempt to give a positive answer to this question in the particular case related to the combinatorics of multitriangulations of a convex polygon (the multiassociahedron). Unfortunately, this attempt failed, but the brick polytope still has many interesting properties.

If the brick polytope has dimension $m - \binom{n}{2}$, the answer is yes, by the construction of the brick polytope [PS12, Question 2.2]. By [PS12, Question 3.26], there is also another affirmative answer to this question: For a minimal irreducible sorting network \mathcal{N} , the simplicial complex $\Delta(\mathcal{N})$ is the boundary complex of the polar of the brick polytope $\Omega(\mathcal{N})$.

Everything we have seen for sorting networks can be transmitted to triangulations of a convex polygon in some particular cases. We describe a duality between triangulations of a convex polygon and the pseudoline arrangements supported by the 1-kernel (described below) of a reduced alternating sorting network. This duality is used to show that the brick polytopes of reduced alternating² sorting networks specialize to Hohlweg and Lange’s construction of the associahedra.

We give a short description of the constructed convex polygon: \mathcal{P}_x denotes the n -gon for $x \in \{a, b\}^{n-2}$ obtained by the convex hull of $p_1 = (1, 0)$, $p_n = (n, 0)$ and p_{i+1} the point on the circle of diameter $[p_1, p_n]$ with abscissa $i + 1$ and located above $[p_1, p_n]$ if $x_i = a$ and otherwise below, for $i \in [n - 2]$. \mathcal{N}_x denotes the reduced alternating sorting network such that the $(i + 1)$ -th pseudoline touches its top level if $x_i = a$ and its bottom level for all $i \in [n - 2]$. We denote by \mathcal{N}^1 the 1-kernel of a network \mathcal{N} , which is obtained from \mathcal{N} by erasing its first and last level, as well as all commutators incident to them. Now we can observe that the network \mathcal{N}_x^1 has $n - 2$ levels and $\binom{n}{2} - n$ commutators. The binomial coefficient follows by the definition of reduced,

² This is a sorting network with commutators in alternating order, above and below, for each level.

alternating sorting networks and we subtract n commutators since every pseudoline touches the top or bottom level once. For $1 \leq i < j \leq n$, we denote by (i, j) the diagonal or boundary edge $[p_i, p_j]$ of \mathcal{P}_x , and the commutator of \mathcal{N}_x where the i -th and j -th pseudoline of the unique pseudoline arrangement supported by \mathcal{N}_x cross. Note that the commutators bounding the top or bottom level correspond to the boundary edges of the polygon and the remaining commutators are labelled by the internal diagonals of \mathcal{P}_x . An example is illustrated in Figure 2.9. Details are described by Pilaud and Pocchiola in [PS12].

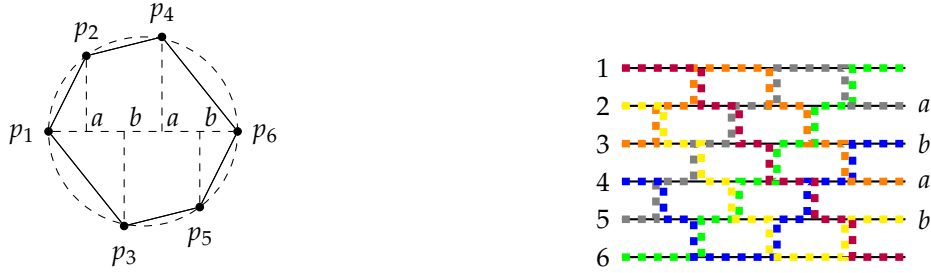


Figure 2.9: Left: \mathcal{P}_{abab} , Right: \mathcal{N}_{abab}

The duality works as follows: The set of commutators of \mathcal{N}_x^1 labelled by the internal diagonals of a triangulation T of \mathcal{P}_x is the set of contacts of a pseudoline arrangement T^* supported by \mathcal{N}_x^1 . Reciprocally, the internal diagonals of \mathcal{P}_x which label the contacts of a pseudoline arrangement supported by \mathcal{N}_x^1 form a triangulation of \mathcal{P}_x . So the dual pseudoline arrangement T^* of a triangulation T of \mathcal{P}_x has one pseudoline Δ^* dual to each triangle Δ of T . Moreover, a commutator is the crossing between two pseudolines Δ^* and Δ'^* of T^* , if it is labelled by the common bisector of the triangles Δ and Δ' . This is illustrated in Figure 2.10.

Remark 2.5: Duality between pseudoline arrangements supported by \mathcal{N}_{abab}^1 and triangulations of \mathcal{P}_{abab} [PS12]

triangulation T of $\mathcal{P}_{abab} \leftrightarrow$ pseudoline arrangement T^* supported by \mathcal{N}_{abab}^1

triangle Δ in $T \leftrightarrow$ pseudoline Δ^* of T^*

common edge of two triangles Δ and $\Delta' \leftrightarrow$ contact between the pseudolines Δ^* and $(\Delta')^*$

common bisector of two triangles Δ and $\Delta' \leftrightarrow$ flip between the pseudolines Δ^* and $(\Delta')^*$

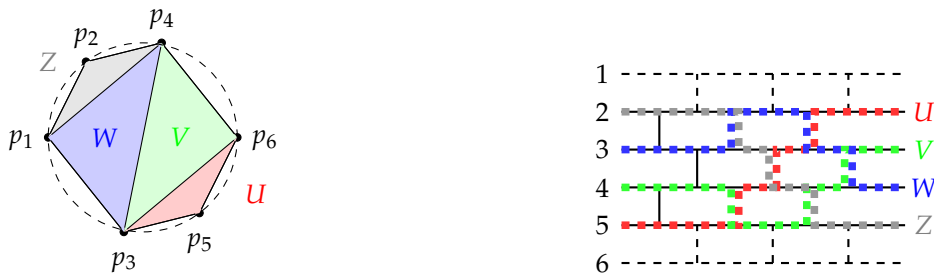


Figure 2.10: Left: triangulation of \mathcal{P}_{abab} , Right: pseudoline arrangement of \mathcal{N}_{abab}^1 for the triangulation on the left.

We also obtain an isomorphism between the graph of flips on pseudoline arrangements supported by \mathcal{N}_x^1 and the graph of flips on triangulations of \mathcal{P}_x . If we consider a triangulation T of \mathcal{P}_x , the contact graph $(T^*)^\#$ of the dual pseudoline arrangement is exactly the dual tree of T , with some additional orientations on the edges. This has been extended by Pilaud and Pocchiola in two

ways: On the one hand to pseudotriangulations of point sets in general position, and on the other hand to multistriangulations of a convex polygon. For details we refer to [PS12].

From this we can get an intuitive understanding of the brick polytope defined by some triangulation of the brick polytope! By the discussed results we see, if \mathcal{N}_x is a reduced alternating sorting network with n levels. Its 1-kernel \mathcal{N}_x^1 is a minimal network: the pseudoline arrangements it supports correspond to triangulations of \mathcal{P}_x and their contact graphs are the dual trees of these triangulations. The main result we have seen is that the brick polytope $\Omega(\mathcal{N}_x^1)$ is a realization of the $(n - 3)$ -dimensional associahedron. Furthermore, these brick polytopes are precisely the associahedra of Hohlweg and Lange [PS12]. It can be seen that, $\Omega(\mathcal{N}_x^1)$ does not depend on the first and last letter. Moreover, a network \mathcal{N}_x and its reflection through the vertical (resp. horizontal) axis give rise to affinely equivalent associahedra, see [PS12] for more details.

Remark 2.6

Hohlweg and Lange's associahedra is not the only one realized by the brick polytope. The brick polytope of the 1-kernel of the network $\mathcal{N}_{b^{n-2}}$ coincides with the $(n - 3)$ -dimensional associahedron of Loday. Another example is Hohlweg and Lange's realization of the cyclohedron. For this they considered the antisymmetric word $x \in \{a, b\}^{2n-2}$ satisfying $\{x_i, x_{2n-1-i}\} = \{a, b\}$, such that the $(2n)$ -gon \mathcal{P}_x is centrally symmetric. Then the convex hull of the brick vectors of the dual pseudoline arrangements of all centrally symmetric triangulations of \mathcal{P}_x is a realization of the $(n - 1)$ -dimensional cyclohedron [PS12].

2.2 Brick polytopes of spherical subword complexes

We start with introducing subword complexes in the context of Coxeter groups as a generalization of the simplicial complex $\Delta(\mathcal{N})$ of a sorting network \mathcal{N} . To remember, the length $\ell(w)$ of an element $w \in W$ is the smallest length of a word $w = (s_1, \dots, s_{\ell(w)})$ such that its product is an expression for w . If $\ell(w)$ is minimal, we call this a reduced expression for w .

Definition 2.7: Subword complex $\mathcal{SC}(Q, w)$ [PS15]

For a Coxeter system (W, S) , let $Q = (q_1, \dots, q_m)$ be a word in the generators S of W and let $\pi \in W$. The subword complex $\mathcal{SC}(Q, w)$ is defined as the simplicial complex whose facets are subsets $I \subseteq [m]$ such that $Q_{[m] \setminus I}$ is a reduced expression for w . Here Q_J denotes the subword of Q with positions at J .

Two facets I and J of $\mathcal{SC}(Q, w)$ are adjacent, if there are $i \in I$ and $j \in J$ such that $I \setminus \{i\} = J \setminus \{j\}$. We call the transition from I to J the flip of $i \in I$ and furthermore say the flip is increasing if $i < j$ and otherwise decreasing. Moreover, we define $\mathcal{SC}(Q) := \mathcal{SC}(Q, w_\circ)$.

The simplicial complex $\Delta(\mathcal{N})$ can be naturally obtained as a subword complex $\mathcal{SC}(Q_{\mathcal{N}}, w_\circ)$ with underlying Coxeter group $(\mathfrak{S}_n, \{s_i \mid i \in [n - 1]\})$ and the permutation $w_\circ := [n, n - 1, \dots, 2, 1]$ the longest element of \mathfrak{S}_n . A commutator connecting levels i and $i + 1$ in \mathcal{N} corresponds to a letter s_i in $Q_{\mathcal{N}}$, and these letters are read from left to right in the network. The contacts of a pseudoline arrangement supported by \mathcal{N} correspond to a facet of $\mathcal{SC}(Q_{\mathcal{N}}, w_\circ)$, and vice versa. Therefore the simplicial complex $\Delta(\mathcal{N})$ is isomorphic to $\mathcal{SC}(Q_{\mathcal{N}}, w_\circ)$.

Having considered the case of sorting networks of the form $\mathcal{SC}(Q, w_\circ)$, we go one step further and generalize the brick polytope to spherical subword complexes. By [KM04, Corollary 3.8] a subword complex $\mathcal{SC}(Q, w)$ is spherical if and only if $\text{Dem}(Q) = w$, otherwise a ball. $R(I)$ of a facet I , or equivalently of all facets, is linearly independent. In the case where the root configuration $R(I)$ of a facet I , or equivalently of all facets, is linearly independent, then the polar of the brick polytope is a realization of the subword complex, by [PS15].

In this thesis, we always consider the Coxeter system (W, S) of type A_n : $W := S_{n+1}$ which is acting on $V := \{x \in \mathbb{R}^{n+1} \mid x_1 + \dots + x_{n+1} = 0\}$ by permutation of coordinates, $S := \{s_p \mid p \in [n]\}$ with $s_p = (p, p+1)$ and $\Phi = \{e_p - e_q \mid p \neq q \in [n+1]\} = \Phi^+ \sqcup \Phi^-$ with $\Phi^+ = \{(e_i - e_j) \mid 1 \leq i < j \leq n+1\}$ and $\Phi^- = \{(e_j - e_i) \mid 1 \leq i < j \leq n+1\}$, simple roots $\Delta = \{e_p - e_{p+1} \mid p \in [n]\}$ and fundamental weights $\nabla = \{\sum_{q \leq p} e_q \mid p \in [n]\}$.

Remark 2.8

Note that the fundamental weights we are using are not the same we discussed in Example 1.7 and 1.8. In particular the fundamental weights ∇ do not lie in the vector space V and do not coincide with our original definition of fundamental weights. However, by [PS15, Example 2.2], this alters the definition of the brick polytope below only by a shift, and enables us to match the presentation of the brick polytopes for sorting networks.

Question 2.4 above can be formulated more generally, whether any spherical subword complex is the boundary complex of a convex simplicial polytope [KM04]. This question is widely open. Pilaud and Stump have generalized the construction of the brick polytope on any Coxeter system. This construction yields in particular the generalized associahedra of Hohlweg and Lange [HL07] for certain particular subword complexes described by Ceballos, Labbé and Stump [CLS14].

There will be two important functions, which we are going to define now for $w \in W$ and $Q = (s_1, \dots, s_m)$. The root function $r(I, \cdot) : [m] \rightarrow \Phi$ is defined by $r(I, k) := \prod_{Q_{\{1, \dots, k-1\} \setminus I}}(\alpha_{s_k})$. Therefore we denote by $R(I) := \{r(I, i) \mid i \in I\}$ the root configuration of a facet I . The other function is the weight function $w(I, \cdot) : [m] \rightarrow \Phi$, defined by $w(I, k) := \prod_{Q_{\{1, \dots, k-1\} \setminus I}}(\omega_{s_k})$. Note that the only difference is in the argument. The root function operates on simple roots and the weight function operates on fundamental weights. The following result is proven by Knutson and Miller:

Lemma. 2.9: [KM04]

Let $I \in \mathcal{SC}(Q, w)$ be a facet then $i \in I$ is flippable if and only if

- $r(I, i) \in \text{Inv}(w)$, or
- $r(I, i) \in \Phi^-$

We associate to a word $Q = (q_1, \dots, q_m)$ in S a sorting network \mathcal{N}_Q with $n+1$ levels and m commutators, such that if $q_i = s_p$ then the i -th commutator is between level p and $p+1$.

Example 2.10: \mathcal{N}_Q for $Q = (s_1, s_1, s_2, s_2, s_1, s_1)$

To illustrate this, we can consider the case $n = 2$ and the word $Q = (s_1, s_1, s_2, s_2, s_1, s_1)$, where we are going to write it as $Q = 112211$ for simplicity. The sorting network \mathcal{N}_Q is equal to the sorting network discussed in Example 2.2, shown in Figure 2.3. The set of positive roots is given by $\Phi^+ = \{e_1 - e_2, e_1 - e_3, e_2 - e_3\}$. We observe two properties, which hold in general, namely $|I^c| = |Q \setminus I|$ and $|I^c| = |\Phi^+|$. These observations are formulated by the next Lemma.

Lemma. 2.11: [PS15]

Let I be a facet of the subword complex $\mathcal{SC}(Q)$.

- The map $r(I, \cdot) : k \mapsto r(I, k)$ determines a bijection between the complement of I and Φ^+ .
- For I, J adjacent facets of $\mathcal{SC}(Q)$ with $I \setminus \{i\} = J \setminus \{j\}$ the position j is the unique position in the complement of I for which $r(I, j) \in \{\pm r(I, i)\}$. Moreover, $r(I, j) = r(I, i) \in \Phi^+$ if $i < j$ and $r(I, j) = -r(I, i) \in \Phi^-$ if $i > j$.
- In the same situation as in the second point, the map $r(J, \cdot)$ is obtained from the map $r(I, \cdot)$ by

$$r(J, k) = \begin{cases} s_{r(I, i)}(r(I, k)) & \text{if } \min(i, j) < k \leq \max(i, j) \\ r(I, k) & \text{otherwise} \end{cases}$$

We say a root configuration $R(I)$ for a facet I of a subword complex is root independent if $R(I)$ is a set of linearly independent vectors. By Lemma 2.11, either all the root configurations $R(I)$ for facets I of $\mathcal{SC}(Q)$ are simultaneously linearly independent, or none of them is. For more details we refer to [PS15, Lemma 3.8].

Definition 2.12: Brick polytope [PS15]

For a spherical subword complex $\mathcal{SC}(Q)$, with $Q = (q_1, \dots, q_m)$, $\text{Dem}(Q) = w_\circ$ and weight function $w(I, k) = \prod_{Q_{\{1, \dots, k-1\} \setminus I}(\omega_{s_k})}$, define the brick vectors $B(I) := \sum_k w(I, k)$ and the brick polytope as the convex hull of the brick vectors:

$$\mathcal{B}(Q) := \text{conv}\{B(I) \mid I \text{ facet of } \mathcal{SC}(Q)\} = \text{conv}_I B(I).$$

Example 2.13

We continue Example 2.10, the facets are: $I_1 = (1, 3, 5)$, $I_2 = (2, 3, 5)$, $I_3 = (2, 4, 5)$, $I_4 = (2, 4, 6)$, $I_5 = (1, 4, 6)$, $I_6 = (1, 3, 6)$, $I_7 = (2, 3, 6)$, $I_8 = (1, 4, 5)$. We are going to compute the weight function explicitly:

The fundamental weights are given by: $\omega_1 = e_1$, $\omega_2 = e_1 + e_2$.

The simple roots are: $\alpha_1 = e_1 - e_2$, $\alpha_2 = e_2 - e_3$.

We do the calculation for facet I_1 explicitly:

$$\begin{aligned} w(I_1, 1) &= \omega_1 = e_1, & w(I_1, 2) &= \omega_1 = e_1, & w(I_1, 3) &= s_1(\omega_2) = e_1 + e_2, \\ w(I_1, 4) &= s_1(\omega_2) = e_1 + e_2, & w(I_1, 5) &= s_1 s_2(\omega_1) = e_2, & w(I_1, 6) &= s_1 s_2(\omega_1) = e_2, \end{aligned}$$

Therefore, $b(I_1) = \sum w(I_1, k) = 4(e_1 + e_2) = (4, 4, 0)^\top$. Here is the list of all brick vectors:

$$\begin{aligned} b(I_1) &= (4, 4, 0)^\top, & b(I_2) &= (3, 5, 0)^\top, & b(I_3) &= (2, 5, 1)^\top, & b(I_4) &= (2, 4, 2)^\top, \\ b(I_5) &= (3, 3, 2)^\top, & b(I_6) &= (4, 3, 1)^\top, & b(I_7) &= (3, 4, 1)^\top, & b(I_8) &= (3, 4, 1)^\top \end{aligned}$$

The computation of the root configuration works similar. We do the calculation for facet I_1 explicitly:

$$\begin{aligned} r(I_1, 1) &= \alpha = e_1 - e_2, & r(I_1, 2) &= \alpha_1 = e_1 - e_2, & r(I_1, 3) &= s_1(\alpha) = e_1 - e_3, \\ r(I_1, 4) &= s_1(\alpha) = e_1 - e_3, & r(I_1, 5) &= s_1 s_2(\alpha_1) = e_2 - e_3, & r(I_1, 6) &= s_1 s_2(\alpha_1) = e_2 - e_3, \end{aligned}$$

Therefore, $R(I_1) = \{e_1 - e_2, e_1 - e_3, e_2 - e_3\}$.

Remark 2.14

Notice that the computed brick vectors in Example 2.13 do not coincide with those from Example 2.2. By Definition 2.12, the left unbounded brick is counted. However, the resulting brick polytope is just a translation of the one computed before. The precise translation is given by adding the vector $(n-1, n-2, \dots, 0)^\top$ to the brick vectors in Definition 2.1. In particular, the brick vectors in Example 2.13 are obtained from the brick vectors in Example 2.2 by just adding the vector $(2, 1, 0)$ to each of them.

This generalization in Definition 2.12 satisfies the following property, which we have also seen for brick polytopes for sorting networks, in the following way:

Proposition. 2.15: [PS15]

Let I be a facet of the subword complex $\mathcal{SC}(Q)$. The cone of the brick polytope at the brick vector $B(I)$ coincides with the cone generated of the negative of the root configuration of I :

$$\text{cone}\{B(J) - B(I) \mid J \text{ facet of simplicial complex } \mathcal{SC}(Q)\} = \text{cone}\{-r(I, i) \mid i \in I\}.$$

2.3 Brick polyhedra

Now our task is to come up with a generalization of the brick polytopes for spherical subword complexes towards general subword complexes by introducing brick polyhedra [JS23]. We start by giving a connection between Bruhat intervals in finite Coxeter groups and subword complexes. At the end we combine Bruhat cones with brick polytopes to define brick polyhedra for all subword complexes. Some statements for brick polytopes will also hold for brick polyhedra and others can be adapted. First, our aim in this section is to give a brief introduction about the connection between Bruhat intervals and subword complexes.

Definition 2.16: Bruhat cone [JS23]

For a Bruhat interval $[x, y]$, the upper Bruhat cone is defined by $\mathcal{C}^+(x, y) := \text{cone } \mathcal{E}^+(x, y)$, the lower Bruhat cone $\mathcal{C}^-(x, y) := \text{cone } \mathcal{E}^-(x, y)$, where $\mathcal{E}^+(x, y) := \{\beta \in \Phi^+ \mid x \prec_B s_\beta x \leq_B y\}$ and $\mathcal{E}^-(x, y) := \{\beta \in \Phi^+ \mid x \leq_B s_\beta y \prec_B y\}$, which only means that the upper Bruhat cone is the cone spanned by the labels of the atoms in the Bruhat interval $[x, y]$. If we write Bruhat cone, we talk about the upper Bruhat cone.

Remark 2.17: Making-of the definition of the Bruhat Cone

Behind this definition there is the following idea: In the case that we have a non-flippable $i \in I \in \mathcal{SC}(Q)$ the root $r(I, i)$ is still a positive root that does not belong to the inversion set, $r(I, i) \in \Phi^+ \setminus \text{Inv}(w)$. In terms of the Demazure product, we can insert the generator q_i into the reduced word of w determined by the complement of I and get $w \prec_B r_\beta w \leq_B \text{Dem}(Q)$, where $\beta = r(I, i)$. This insertion/deletion of letters yields a connection between the subword complexes $\mathcal{SC}(Q, r_\beta w) \leftrightarrow \mathcal{SC}(Q, w)$. So we can consider all of these upper covers that are still below $\text{Dem}(Q)$. This leads us to the Bruhat cones. Especially, if we have an interval $x \leq_B y$ for $x, y \in W$, we consider an upper cover of x in Bruhat order $x \prec_B z \leq_B y$, such an upper cover corresponds to a reflection $r \in \mathcal{R}$, such that $rx = z$ and this reflection has a corresponding positive root $\beta \in \Phi^+$, i.e. $r = r_\beta$.

Now we collect for the interval $[x, y]$ all such roots β and define $\mathcal{E}^+(x, y) = \{\beta \in \Phi^+ \mid x \prec_B r_\beta x \leq_B y\}$, which gives us some rays. The Bruhat cone is the cone over those roots $\mathcal{C}^+(x, y) = \text{cone } \mathcal{E}^+(w, \text{Dem}(Q))$. By [JS23], the following holds:

Theorem 2.18: [JS23]

Let $\mathcal{SC}(Q, w)$ be a non-empty subword complex. Then

$$\mathcal{C}^+(w, \text{Dem}(Q)) = \bigcap_{I \text{ facet of } \mathcal{SC}(Q, w)} \text{cone } R(I), \quad (2.1)$$

$$\mathcal{E}^+(w, \text{Dem}(Q)) = \{r(I, i) \mid I \text{ facet of } \mathcal{SC}(Q, w) \text{ and } i \in I \text{ non-flippable}\}. \quad (2.2)$$

Moreover, if for a facet I of $\mathcal{SC}(Q, w)$, $i \in I$ is a flippable index, then $r(I, i) \notin \mathcal{E}^+(w, \text{Dem}(Q))$.

Theorem 2.18 states that we can describe the root function values of all non-flippable indices exactly by these sets of roots that correspond to upper covers. Now we reduce our studies to simplicial complexes containing non-flippable vertices. This happens when

$$\begin{aligned} \mathcal{E}^+(w, \text{Dem}(Q)) \neq \emptyset &\Leftrightarrow w < \text{Dem}(Q) \\ &\Leftrightarrow \mathcal{SC}(Q, w) \text{ is a ball} \\ &\Leftrightarrow \mathcal{SC}(Q, w) \text{ has facets containing non-flippable vertices} \end{aligned}$$

Definition 2.19: Brick polyhedra [JS23]

The brick vector of a facet $I \in \mathcal{SC}(Q, w)$ for a word $Q = (q_1, \dots, q_m)$ is defined by $b(I) := -\sum_{k=1}^m w(I, k)$. (The minus sign simplifies the notation in later aspects.) The brick polyhedron $\mathcal{B}(Q, w)$ of a non-empty subword complex $\mathcal{SC}(Q, w)$ is the Minkowski sum of the convex hull of all brick vectors and the Bruhat cone $\mathcal{C}^+(w, \text{Dem}(Q))$:

$$\mathcal{B}(Q, w) := \text{conv}\{b(I) \mid I \text{ facet of } \mathcal{SC}(Q, w)\} + \mathcal{C}^+(w, \text{Dem}(Q)).$$

Definition 2.19 coincides with the brick polytope in the spherical case (for $w = \text{Dem}(Q)$), because then the Bruhat cone is just a point. Now, how does the added cone influence the structure of the brick polytope? The brick polyhedron preserves many of the properties of the brick polytope, one reason for this is that the Bruhat cone $\mathcal{C}^+(w, \text{Dem}(Q))$ is exactly the intersection of all cones over root configurations. The Bruhat cone is given by $\mathcal{C}^+(w, \text{Dem}(Q)) = \{0\}$ if and only if $\text{Dem}(Q) = w$, which is equivalent to the subword complex $\mathcal{SC}(Q, w)$ being spherical. Equivalently, the brick polyhedron $\mathcal{B}(Q, w)$ of a non-empty subword complex $\mathcal{SC}(Q, w)$ is polytopal³ if and only if $\mathcal{SC}(Q, w)$ is spherical. Our definition of the brick polyhedra allows us to keep the following local property, shown in [JS23]. What can go wrong is given in Example 2.23.

Definition 2.20: Local cone [JS23]

The local cone of a polyhedron P at a point $q \in P$ is defined by

$$\text{cone}^{(q)}(P) := \text{cone}\{p - q \mid p \in P\}.$$

³ We call a bounded polyhedron polytopal. P is called a polyhedron if there are finitely many linear functions $f_1, \dots, f_k : V \rightarrow \mathbb{R}$ and scalars $b_1, \dots, b_k \in \mathbb{R}$ such that $P = \{v \in V : f_i(v) + b_i \geq 0 \text{ for all } 1 \leq i \leq k\}$.

Theorem 2.21: [JS23]

The local cone of the brick polyhedron $\mathcal{B}(Q, w)$ at the brick vector $b(I)$ coincides with the cone generated by the root configuration of the facet I of $\mathcal{SC}(Q, w)$. In symbols:

$$\text{cone}^{(b(I))}(\mathcal{B}(Q, w)) = \text{cone } R(I).$$

As an immediate consequence we obtain Corollary 2.22.

Corollary 2.22: [JS23]

For I, J facets of a subword complex $\mathcal{SC}(Q, w)$ such that their brick vectors $b(I)$ and $b(J)$ are contained in the same edge of the brick polyhedron $\mathcal{B}(Q, w)$, then the facets I, J are connected by a flip.

In the following example we can see, if we only take the convex hull of the brick vectors and draw the corresponding root configuration with vectors, there are vertices such that the root configuration lies outside the polytope. Taking the Minkowski sum with the Bruhat cone is fixing this, as Example 2.23 shows.

Example 2.23

(Type A_2) Let $Q = (s_2, s_1, s_2, s_1)$ and $w = s_2 s_1$. The subword complex $\mathcal{SC}(Q, w)$ has three facets $I_1 = (1, 2)$, $I_2 = (2, 3)$, $I_3 = (3, 4)$ with corresponding brick vectors $b(I_1) = -(0, 2, 4)^\top$, $b(I_2) = -(0, 3, 3)^\top$, $b(I_3) = -(1, 3, 2)^\top$. The subword complex is non-spherical since $\text{Dem}(Q) = s_2 s_1 s_2 \neq w$, and root dependent. The corresponding brick polyhedron is shown in Figure 2.11. The local cone of the brick polytope, using only the convex hull, does not coincide with the cone spanned by the root configuration at the brick vector for the facets I_1 and I_3 . The solution for this is to add the so-called Bruhat cone in the sense of a Minkowski sum, discussed above.



Figure 2.11: Left: Sorting network \mathcal{N}_Q for $Q = (s_2, s_1, s_2, s_1)$, Right: Brick vectors and root configuration

After introducing brick polyhedra we give a brief introduction of the normal fans of brick polyhedra. [JS23, Corollary 4.18].

Definition 2.24: Coxeter fan [JS23]

The Coxeter fan of a Coxeter group W is defined by $\mathcal{CF}_W = \{w(\text{cone } \nabla') \mid w \in W, \nabla' \subseteq \nabla\}$ with the fundamental chamber $\mathcal{C} = \text{cone}(\nabla)$ being the cone spanned by the fundamental weights.

Definition 2.25: [JS23]

For a Bruhat interval $[x, y]$ define the ideal $Id_R(x, y) := \{z \in W \mid \mathcal{E}^+(x, y) \subseteq z(\Phi^+)\}$ and the map $\kappa : Id_R(w, \text{Dem}(Q)) \rightarrow \mathcal{SC}(Q, w)$, by sending $z \in Id_R(w, \text{Dem}(Q))$ to the unique facet I_f with $R(I) \subseteq z(\Phi^+)$. Here f is the linear functional, which is positive on $z(\Phi^+)$ and negative on $z(\Phi^-)$ and I_f is the unique facet for which $R(I) \subseteq z(\Phi^+)$.

By [JS23, Proposition 4.12], the map κ is well defined and by [JS23, Proposition 4.16] surjective. We also have Corollary 2.26

Corollary 2.26: [JS23]

The normal fan $\mathcal{N}(\mathcal{B}(Q, w))$ is obtained from the Coxeter fan by glueing together the chambers corresponding to fibers of the map κ , and deleting the chambers corresponding to elements in w not in $Id_R(w, \text{Dem}(Q))$.

Example 2.27: Normal fan

We consider the subword complex $\mathcal{SC}(Q, w)$ with $Q = (s_2, s_1, s_3, s_2)$ and $w = s_2$. The simple roots are $\Phi^+ = \{(e_i - e_j) | 1 \leq i < j \leq 4\}$. Let I_2 be the greedy facet and I_1 the anti-greedy facet. The brick polyhedron $\mathcal{B}(Q, w)$ is given by the two brick vectors $b(I_1), b(I_2)$ connected by a flip, such that $b(I_2) - b(I_1) = e_2 - e_3$. By Theorem 2.18, the Bruhat cone is spanned by the elements $\mathcal{E}^+(w, \text{Dem}(Q)) = \{e_1 - e_2, e_3 - e_4, e_1 - e_3, e_2 - e_4\}$.

We obtain $Id_R(w, \text{Dem}(Q)) = \{w \in W | \mathcal{E}^+(w, \text{Dem}(Q)) \subseteq z(\Phi^+)\} = \{e, s_2\}$. By Corollary 2.26 the normal fan is given by $\mathcal{N}(\mathcal{B}(Q, w)) = \{\{\omega_1\}, \{\omega_2\}, \{\omega_3\}, \{s_2\omega_2\}, \{\omega_1, \omega_2\}, \{\omega_2, \omega_3\}, \{\omega_1, \omega_3\}, \{\omega_1, s_2\omega_1\}, \{\omega_3, s_2\omega_2\}, \{\omega_1, \omega_2, \omega_3\}, \{\omega_1, s_2\omega_2, \omega_3\}\}$, illustrated in Figure 2.13. The interior of the normal fan $\mathcal{N}(\mathcal{B}(Q, w))$ is given by $\{\{\omega_1, \omega_3\}, \{\omega_1, \omega_2, \omega_3\}, \{\omega_1, \omega_3, s_2(\omega_2)\}\}$.

Since the sorting network \mathcal{N}_Q is embedded in the sorting network of Figure 2.8 (Left), the bounded faces of the brick polyhedron $\mathcal{B}(Q, w)$ and the directions of the Bruhat cone are embedded in the permutahedron of order four. This embedding is shown in Figure 2.12: The arrows mark the directions of the Bruhat cone. The corresponding vectors of the normal fan are denoted by the orange letters. Note this coincides with $\omega_i \perp (e_j - e_{j+1})$ for $i \neq j$.



Figure 2.12: Left: Embedding of the sorting network \mathcal{N}_Q in the sorting network in Figure 2.8, Right: Embedding of the brick polyhedron $\mathcal{B}(Q, w)$ in the permutahedron of order four with $Q = (s_2, s_1, s_3, s_2)$ and $w = s_2$.

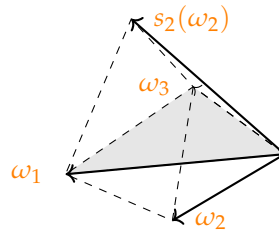


Figure 2.13: Normal fan of the brick polyhedron $\mathcal{B}(Q, w)$ with $Q = (s_2, s_1, s_3, s_2)$ and $w = s_2$.

3 Application

After studying brick polytopes and generalizing them to brick polyhedra, we will introduce the ν -Tamari lattice and project brick polyhedra in a nice way to obtain ν -Tamari lattices. This means we will apply our results to give geometric realizations of ν -associahedra by brick polyhedra.

3.1 The ν -Tamari lattice

We denote by ν a lattice path with finitely many East and North steps. Let F_ν be the Ferrers diagram weakly above ν , inside the smallest rectangle containing ν . A_ν is the set of lattice points weakly above ν , which are inside F_ν . We consider all paths weakly above ν with the same starting and endpoint in A_ν . We define the ν -Tamari lattice as the poset T_ν on this set of paths with a covering relation \prec_ν . The cover relation is given by [CPS20] as follows:

For $p \in A_\nu$, define the $\text{arm}(p)$ to be the maximum number of East steps that can be added to p without crossing ν . Let u be a lattice path weakly above ν . Suppose for an integer point p on u , it is preceded by an East step and followed by a North step in u . Let p_0 be the first lattice point in u which is after p and such that $\text{arm}(p_0) = \text{arm}(p)$. Let $P[p, p_0]$ be the subpath of u that starts at p and finishes at p_0 . Let u_0 be obtained from u by switching E and $P[p, p_0]$. This cover relation is denoted by \prec_ν and its induced poset is called the ν -Tamari lattice. Figure 3.1 shows an example of the cover relation and Figure 3.30 (Left) shows an example of the ν -Tamari lattice for $\nu = EENEEN$.

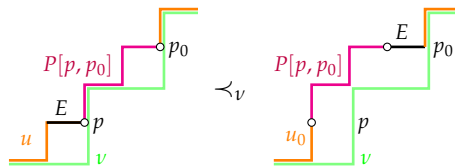


Figure 3.1: Example cover relation: $ENENENENE = u \prec_\nu u_0 = ENNENEENE$.

In the following, we will introduce ν -trees and its rotation lattice. Let $p, q \in A_\nu$. We say p and q are ν -incompatible $p \not\prec q$ if and only if p is southwest (SW) to q or p is northeast (NE) to q and the smallest rectangle containing p, q is completely inside F_ν . A ν -tree is a maximal collection of pairwise ν -compatible elements in A_ν . The elements are called nodes. The top left corner is called root. We associate a rooted binary tree τ to each ν -tree T by connecting every $p \in T$ other than the root to the next in North or West direction. An example is illustrated in Figure 3.3. By [CPS19], exactly one exists and the resulting graph is a rooted binary tree. By ν -compatibility a planar drawing of τ is non-crossing, since 2 crossing parent nodes would be ν -incompatible. One can also show that every rooted binary tree τ can be obtained uniquely as the binary tree of a ν -tree

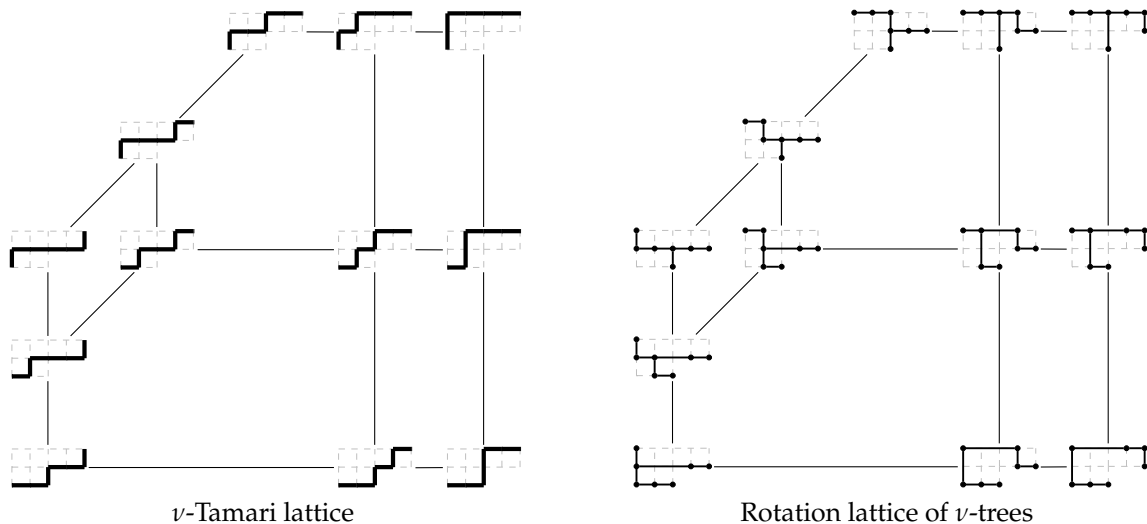


Figure 3.2: Example $\nu = EENEEN$.

T , where ν is uniquely determined by τ [CPS19]. Two ν -trees T, T' are related by a right rotation if T' can be obtained from T by exchanging $q \in T$ with $q' \in T'$ in as in Figure 3.4 with $p, r \in T, T'$.

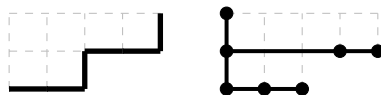


Figure 3.3: Left: $\nu = EENEEN$, Right: ν -tree.

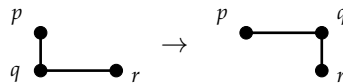


Figure 3.4: Right rotation.

The inverse is called a left rotation. Clearly the rotation of a ν -tree is also a ν -tree. The rotation poset of ν -trees is the partial order on the set of ν -trees, which is defined by the cover relation $T < T'$ if T' can be obtained by a right rotation of T . Moreover, the rotation poset of ν -trees is a lattice, and the rotation poset of ν -trees is connected. All ν -trees have the same number of nodes, which is the number of lattice points on ν . Two ν -trees differ by a single element if and only if they are related by a rotation. More remarkable, the following holds, see example in Figure 3.30:

Theorem 3.1: [CPS19]

The ν -Tamari lattice is isomorphic to the rotation poset of ν -trees.

We present a bijection from [CPS20], which induces an isomorphism between the rotation lattice of ν -trees and the ν -Tamari lattice. We give a short description of the right flush \mathcal{R} , which constructs a ν -tree from a ν -path μ : Start with labeling all points in the ν -path μ in order they appear along the path. Now we are constructing the ν -tree from the bottom to the top. The vertices in a row are placed as rightmost as possible on the same row of the path in assigned order. But we avoid the x -coordinates that are forbidden by previous flushed rows. We disallow here the coordinates by all flushed points in a row, excepting the last one (leftmost). The obtained points give us the ν -tree. The Left flush \mathcal{L} will work symmetrically, see [CPS20]. This bijection is visualized in Figure 3.5. The maps \mathcal{R}, \mathcal{L} are well defined, and bijective inverse to each other. Moreover,

for μ, μ' ν -paths, they are related by a ν -Tamari covering if and only if $\mathcal{R}(\mu')$, $\mathcal{R}(\mu)$ are related by a rotation.

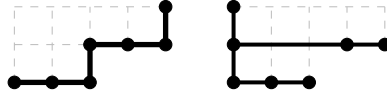


Figure 3.5: \rightarrow Right shift, \leftarrow Left shift.

3.2 The ν -Tamari complex and the ν -subword complex

The description of the ν -Tamari lattice in terms of ν -trees allows us to introduce a much richer structure, called the ν -Tamari complex.

Definition 3.2: ν -Tamari Complex [CPS19]

The ν -Tamari complex is the simplicial complex $\mathcal{TC}(\nu)$ of pairwise ν -compatible sets in A_ν . The dimension of a face I is $\dim(I) = |I| - 1$. The facets are the ν -trees.

As shown in [CPS19], the ν -Tamari complex can be determined as a well chosen subword complex. For this, we need to introduce pipe dreams [Ber+23] and the words Q_ν , w_ν corresponding to a finite path ν .

Definition 3.3: Pipe dream [Ber+23], [CPS19]

A pipe dream P is a filling triangular shape with crosses \vdash and elbows \lrcorner . The permutation of the pipe dream P is denoted by $\pi(P)$, and any two pipes have at most one intersection. To each ν -tree T we associate a pipe dream $P(T)$ by placing elbows at all nodes of the ν -tree and outside F_ν . This is illustrated in Figure 3.7. For a fixed ν the permutation $\pi_\nu := \pi_\nu(T)$ is independent of the ν -tree T , because rotations do not alter the permutation. However, every pipe dream with permutation π_ν arises this way.

Definition 3.4: Q_ν and w_ν [CPS19]

Let ν be a finite path of length n . For every lattice point in the Ferrers diagram $p \in F_\nu$, denote by $d(p)$ the lattice distance from p to the top-left corner of F_ν . Now label each integer lattice point $p \in F_\nu$ by the transposition $s_{d(p)+1}$. See Figure 3.6 (Middle) for an example.

Furthermore, define Q_ν as the word obtained by reading the associated transpositions from bottom to top, and the columns from left to right.

We denote by π_ν the permutation whose one-line representation, denoted with square brackets, is given by the top labels, read from left to right in the corresponding pipe dream. The reduced word w_ν is such that $\pi_\nu = w_\nu(1, \dots, n)$.

Remark 3.5: [CPS19]

The complements of ν -trees are the reduced expressions of w_ν in Q_ν . The effect of a rotation keeps w_ν constant. Figure 3.6 shows an example.

Example 3.6

We consider the path $\nu = ENEEN$. By the Figures 3.6, 3.7 we obtain Q_ν , w_ν , π_ν .

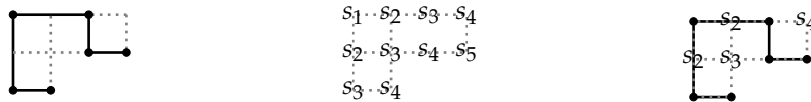


Figure 3.6: Left: ν -tree, Middle: grid for Q_ν Right: complement of ν -tree, $\nu = ENENE$

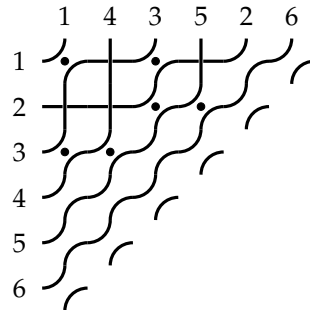


Figure 3.7: Pipe dream for ν -tree, $\nu=ENENE$

By Figure 3.6 (Middle), we obtain $Q_\nu = (s_3, s_2, s_1, s_4, s_3, s_2, s_4, s_3, s_5, s_4)$, Figure 3.6 (Right) gives us $w_\nu = s_2 s_3 s_2 s_4$. The pipe dream in Figure 3.7 illustrates $\pi_\nu = [1, 4, 3, 5, 2, 6]$.

Definition 3.7

The ν -subword complex is the subword complex $\mathcal{SC}(Q_\nu, w_\nu)$.

Theorem 3.8: [CPS19]

The ν -subword complex $\mathcal{SC}(Q_\nu, w_\nu)$ is isomorphic to the ν -Tamari complex.

Definition 3.9: Boundary and Interior of ν -Tamari Complex [CPS19]

A co-dimension 1 face A of the ν -Tamari complex¹ is in the boundary if it is contained in only one facet. A general face B is in the boundary if it is contained in some A of co-dimension 1, which is in the boundary. An interior face is a face that is not in the boundary.

3.3 The ν -associahedron

The Hasse diagram of the ν -Tamari lattice can be geometrically realized as the edge graph of a polytopal complex called the ν -associahedron [CPS19]. The construction in [CPS19] uses techniques from tropical geometry. The goal of this thesis is to give new realizations in terms of brick polyhedra. The following is a purely combinatorial definition.

Definition 3.10: ν -Associahedron [CPS19]

The ν -associahedron is a polytopal complex induced by an arrangement of tropical hyperplanes, whose poset of faces (ordered by containment) is anti-isomorphic to the poset of interior faces of the ν -Tamari complex.

The interior faces of the ν -Tamari complex can be characterized as follows.

¹) The co-dimension of A is given by the maximal dimension minus the dimension of A .

Definition 3.11: [CP20]

A node v in a ν -tree T is called an ascent if there exists a node to the North and another to the East of v . Equivalently, ascents of T are the increasingly flippable nodes of T .

Lemma 3.12: [CP20]

The interior faces I of the ν -Tamari complex are in bijective correspondence with pairs (T, A) , where T is a ν -tree and A is a subset of its ascents, via the map $I = T \setminus A$.

Corollary 3.13: [CP20]

The faces of the ν -associahedron are in correspondence with pairs (T, A) , where T is a ν -tree and A is a subset of its ascents. The dimension of the face corresponding to (T, A) is $|A|$.

Example 3.14

Consider the path $\nu = EN$. We associate to the lattice points in the Ferrers diagram F_ν the letters $\{a, b, c, d\}$, as in Figure 3.8 (Left). By Definition 3.4, we obtain $Q_\nu = (s_2, s_1, s_3, s_2)$ and $w_\nu = s_2$. Therefore, $SC(Q_\nu, w_\nu) = \{abc, bcd, ab, bd, cd, bc, ac, a, b, c, d\}$. The interior faces are $\{abc, bcd, bc\}$. Consequently, by Theorem 3.8, the ν -associahedron is, up to isomorphism, represented by the line segment shown in Figure 3.8 (Right).

We go one step further and consider the sorting network shown in Figure 3.8 (Second left), which has two non-flippable contacts b and c . The corresponding brick polyhedron is shown in Figure 3.9. By Theorem 2.18, the Bruhat cone is of dimension 3, because by Theorem 2.18 (2.2) the Bruhat cone is given by $\mathcal{C}^+(w_\nu, \text{Dem}(Q_\nu)) = \text{cone}\{\alpha_1, \alpha_3, s_2(\alpha_1), s_2(\alpha_3)\}$ and $\alpha_1 + s_2(\alpha_3) = \alpha_3 + s_2(\alpha_1)$. The bounded faces of the ν -brick polyhedron are given by one edge, which we label, $\{bc\}$, between the two possible facets $\{abc\}, \{bcd\}$, see Figure 3.9.

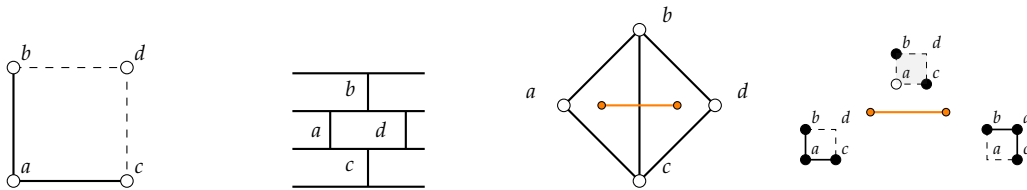


Figure 3.8: From left to right: ν -tree, sorting network, ν -Tamari complex, ν -associahedron

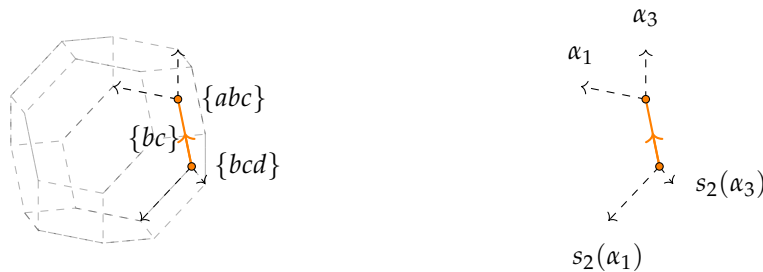


Figure 3.9: ν -Brick Polyhedra for $\nu = EN$

By Example 2.27 the interior of the normal fan $\mathcal{N}(\mathcal{B}(Q_\nu, w_\nu))$ is given by $\{\{\omega_1, \omega_3\}, \{\omega_1, \omega_2, \omega_3\}, \{\omega_1, \omega_3, s_2\omega_2\}\}$.

Example 3.15

Consider the ν -subword complex for $\nu = ENEEN$, the ν -associahedron is shown in Figure 3.10, and its edge graph is the Hasse diagram of the ν -Tamari lattice. The interior face I_1 illustrated in orange in Figure 3.10 corresponds to the orange line segment, while the red interior face I_2 corresponds to the red pentagon. Note that $I_2 \subseteq I_1$, but the face corresponding to I_1 is contained in the face corresponding to I_2 . The containment poset of interior faces is reversed.

The word Q_ν and element w_ν are $Q_\nu = (s_3, s_2, s_1, s_4, s_3, s_2, s_4, s_3, s_5, s_4)$, $w_\nu = s_3 s_2 s_3 s_4$. The brick polyhedron $\mathcal{B}(Q_\nu, w_\nu)$ is of dimension 4 in a 5 dimensional space, so we can not really draw it. However, to get a feeling about how it looks like, we can remove the letters s_1 and s_5 from Q_ν . They are contained in every facet (are non-flippable) and give rays in the brick polyhedron. If we call \tilde{Q}_ν the resulting word $\tilde{Q}_\nu = (s_3, s_2, s_4, s_3, s_2, s_4, s_3, s_4)$ then the brick polyhedron $\mathcal{B}(\tilde{Q}_\nu, w_\nu)$ is of dimension 3 and is illustrated in Figure 3.14. By Theorem 2.18, the Bruhat cone is of dimension 2, because by Theorem 2.18 (2.2) the Bruhat cone is given by $\mathcal{C}^+(w_\nu, \text{Dem}(Q_\nu)) = \text{cone}\{\alpha_4, s_3(\alpha_4)\}$.

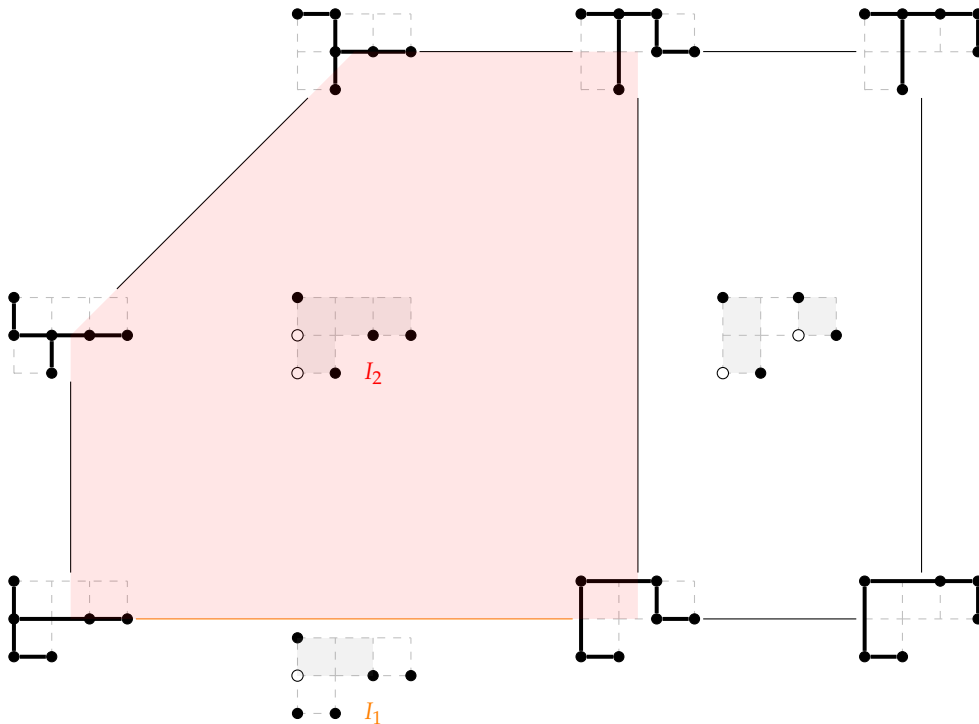


Figure 3.10: The ν -associahedron for $\nu = ENEEN$.

3.3.1 A canonical realization of the alt ν -associahedron

In this subchapter, we define the canonical realization of the alt ν -associahedron.

Definition 3.16: A Canonical Realization of the Alt ν -Associahedron [Ceb24]

For a ν -tree T , the coordinates of the corresponding vertex $x(T)$ in the ν -associahedron are determined as follows: For each horizontal line k in the Ferrer's diagram F_ν , excluding the first one containing the root and labeled from top to bottom, the k -th coordinate of x is given by $x_k(T) = \text{area}(R_k)$. Here, R_k is the shortest path connecting the root to the left most node of T

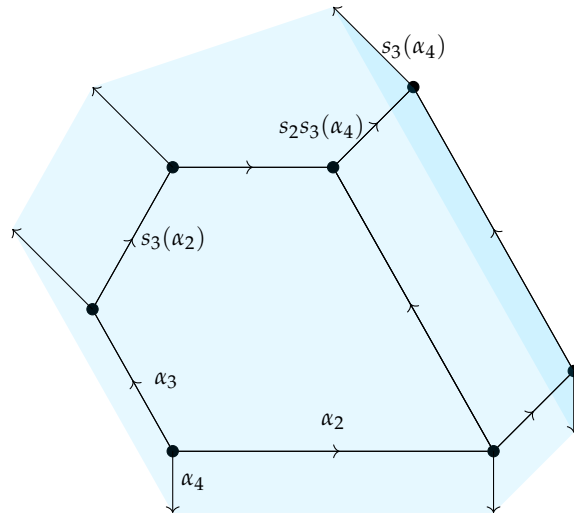


Figure 3.11: $\mathcal{B}(Q_\nu, w_\nu)$ for $\nu = ENEEN$.

on the k -th horizontal line, and $\text{area}(R_k)$ is the number of boxes inside F_ν to the left of R_k . An example is illustrated in Figure 3.12.

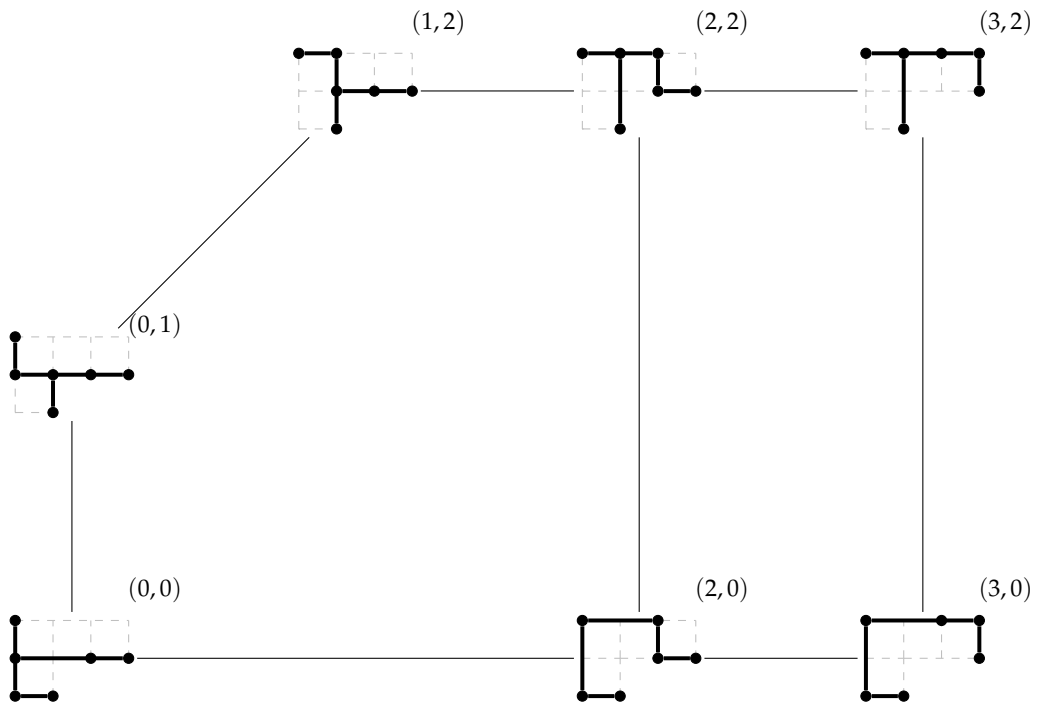


Figure 3.12: The canonical realization of ν -associahedron for $\nu=ENEEN$.

Theorem 3.17: [Ceb24]

The canonical coordinates of ν -trees in Definition 3.16 give a geometric realization of the ν -associahedron.

3.4 A geometric realization via brick polyhedra

In the context of this chapter, we define the ν -brick polyhedron $\mathcal{B}(Q_\nu, w_\nu)$ as the brick polyhedron associated with the ν -subword complex $\mathcal{SC}(Q_\nu, w_\nu)$. Our goal is to demonstrate that the bounded faces of ν -brick polyhedron $\mathcal{B}(Q_\nu, w_\nu)$ also yield a geometric realization of the ν -associahedron, as we can see from Examples 3.14 and 3.15 above.

Theorem 3.18

The bounded faces of the ν -brick polyhedron yield a geometric realization of the ν -associahedron. In other words, the poset of bounded faces of the ν -brick polyhedron is anti-isomorphic to the poset of interior faces of the ν -subword complex ($\cong \nu$ -Tamari complex).

Our approach to establish this result involves the following steps:

- 1) Enhance the understanding of the faces of *general* brick polyhedra (Theorem 3.23).
- 2) Characterize the bounded faces of the ν -brick polyhedron (Corollary 3.45 and Corollary 3.47).
- 3) Analyze the poset of bounded faces of the ν -brick polyhedron (Proof of Theorem 3.18 in Section 3.4.4).

3.4.1 Faces of brick polyhedra

In this chapter, we explore the structure of faces within general brick polyhedra by focusing on identifying the minimal elements within them, as each face contains exactly one minimal element, and characterizing their vertices. We introduce modified brick polyhedra $\mathcal{B}^I(Q, w)$ and demonstrate that every face F of the brick polyhedron $\mathcal{B}(Q, w)$ can be represented as a modified brick polyhedron $\mathcal{B}^I(Q, w)$ for some face $I \in \mathcal{SC}(Q, w)$ (Theorem 3.23).

Definition 3.19: Modified Bruhat Cone $\mathcal{C}^{I,+}$

We denote the set of all faces in the subword complex $\mathcal{SC}(Q, w)$ that contain a given face $I \in \mathcal{SC}(Q, w)$ as $\mathcal{SC}^I(Q, w)$. Formally, we define

$$\mathcal{SC}^I(Q, w) := \{J \in \mathcal{SC}(Q, w) : I \subseteq J\}.$$

The modified root configuration $R^I(J)$ is given by

$$R^I(J) := \{r(J, j) \mid j \in J \setminus I\}.$$

We define the modified Bruhat cone $\mathcal{C}^{I,+}$ as

$$\mathcal{C}^{I,+} := \bigcap_{J \in \mathcal{SC}^I(Q, w)} \text{cone } R^I(J).$$

Definition 3.20: Modified Brick Polyhedron $\mathcal{B}^I(Q, w)$

For a face I of a non-empty subword complex $\mathcal{SC}(Q, w)$, the modified brick polyhedron $\mathcal{B}^I(Q, w)$ is the Minkowski sum of the convex hull of all brick vectors of all facets containing I and the modified Bruhat cone $\mathcal{C}^{I,+}$:

$$\mathcal{B}^I(Q, w) := \text{conv}\{b(J) \mid J \text{ facet of } \mathcal{SC}(Q, w) \text{ and } I \subseteq J\} + \mathcal{C}^{I,+}.$$

Example 3.21

For $\nu = ENEEN$ and using the labeling shown in Figure 3.13, the modified brick polyhedron $\mathcal{B}^{I_2}(Q, w)$ for $I_2 = \{c, d, g, i\}$ is the bounded pentagon in Figure 3.14, while $\mathcal{B}^{I_3}(Q, w)$, where $I_3 = \{a, b, c, i\}$, is not a face of the ν -brick polyhedron $\mathcal{B}(Q, w)$ since it consists of a brick vector and two rays extending to infinity, as illustrated by the red region in Figure 3.14. For $I_4 = \{c, g, h, i\}$, the modified brick polyhedron $\mathcal{B}^{I_4}(Q, w)$ is a slice of the ν -brick polyhedron $\mathcal{B}(Q, w)$, as illustrated by the green region in Figure 3.14.

$$\begin{array}{cccc} c & \cdots & f & \cdots & h & \cdots & j \\ \vdots & & \vdots & & \vdots & & \vdots \\ b & \cdots & e & \cdots & g & \cdots & i \\ \vdots & & \vdots & & \vdots & & \vdots \\ a & \cdots & d & & & & \end{array}$$

Figure 3.13: Grid for labeling of $\mathcal{SC}(Q, w)$ for $\nu = ENEEN$.

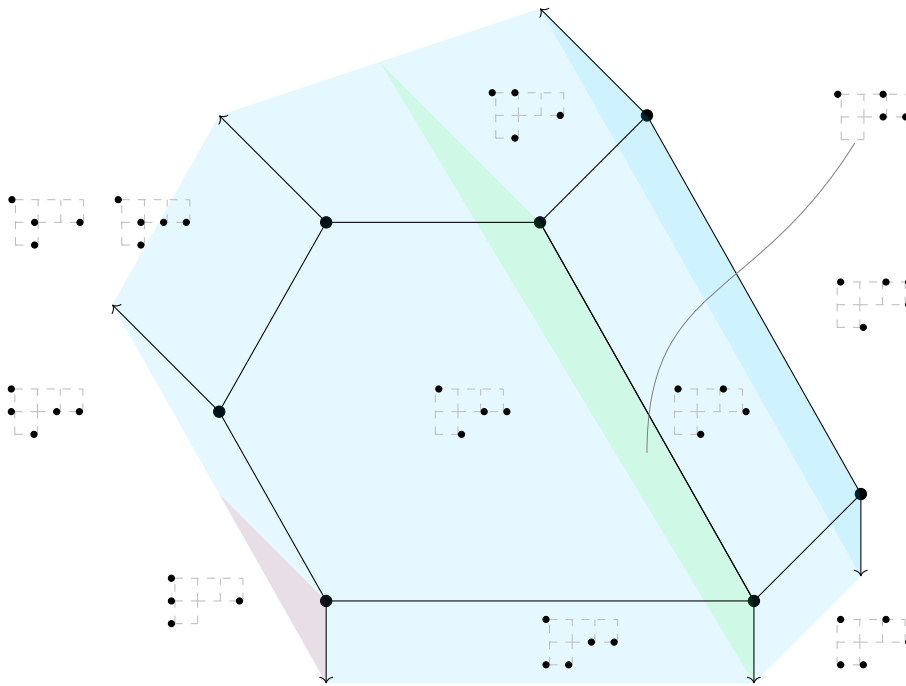


Figure 3.14: $\mathcal{B}(Q, w)$ for $\nu = ENEEN$

Remark 3.22

Note that not every modified brick polyhedron $\mathcal{B}^I(Q, w)$ is a face of the brick polyhedron $\mathcal{B}(Q, w)$, as shown in Example 3.21.

Moving forward, our objective is to establish the following:

Theorem 3.23

Every face F of the brick polyhedron $\mathcal{B}(Q, w)$ is of the form $\mathcal{B}^I(Q, w)$ for some face $I \in \mathcal{SC}(Q, w)$.

Remark 3.24

This result was essentially proved in [JS23] using the description of faces via linear functionals,

see [JS23, Remark 4.11] and [JS23, Corollary 3.24 and Proposition 4.6]. Our approach here is a bit different.

It is essential to develop certain ideas before we can prove Theorem 3.23.

3.4.1.1 The minimal element of a face

First, we demonstrate that each face F of the brick polyhedron $\mathcal{B}(Q, w)$ has a minimal element. To accomplish this, let $\eta \in V$ be a vector such that $\langle \eta, \alpha \rangle > 0$ for $\alpha \in \Phi^+$ and $\langle \eta, \alpha \rangle < 0$ for $\alpha \in \Phi^-$. This vector η can be regarded as a linear functional $\eta : V \rightarrow \mathbb{R}$ defined by $x \mapsto \langle \eta, \beta \rangle$, as established in Remark 1.4. Note $\eta(\alpha) \neq 0$ for all $\alpha \in \Phi$.

Lemma 3.25: Minimal element of a face

For every face F of the brick polyhedron $\mathcal{B}(Q, w)$, there exists a unique vertex $b(J_{F, \min}) \in F$, corresponding to some facet $J_{F, \min}$, that minimizes the linear functional η .

Proof. Let F_η be the sub-face of F that minimizes the linear functional η . We aim to demonstrate that F_η consists of only one point. Otherwise, F_η would contain a (possibly unbounded) edge in the direction of α for some $\alpha \in \Phi$.

Let p and q be two points on this edge such that $q = p + \alpha$ for some $\alpha \in \Phi$. Then, $\langle \eta, q \rangle = \langle \eta, p \rangle + \langle \eta, \alpha \rangle$. Since p and q are minimizing η , it follows that $\langle \eta, \alpha \rangle = 0$, which contradicts to Remark 1.4, which states that $\langle \eta, \alpha \rangle \neq 0$ for all $\alpha \in \Phi$.

□

3.4.1.2 Characterization of the vertices in a face F

In this chapter, we explore how reflections can help characterize the vertices within a face F of the brick polyhedron $\mathcal{B}(Q, w)$. This method offers a straightforward yet powerful way to understand the structure and properties of these vertices. The following Observation 3.26 is a direct consequence of the definition $r_\alpha(\beta) = \beta - 2 \frac{\langle \alpha, \beta \rangle}{\langle \alpha, \alpha \rangle} \alpha$.

Observation 3.26

If $\alpha, \beta \in U$, where U be a finite-dimensional subspace of a vector space, then $r_\alpha(\beta) \in U$. If $\alpha \in U$ and $\beta \notin U$, then $r_\alpha(\beta) \notin U$.

Definition 3.27

Let F be a face in a finite dimensional subspace. The affine vector space \tilde{V}_F is the smallest vector space containing F , while the vector space V_F is obtained by shifting F to the origin.

Lemma 3.28: Characterization of the vertices in a face F

Let F be a face of the brick polyhedron $\mathcal{B}(Q, w)$. Suppose J is a facet of the subword complex $\mathcal{SC}(Q, w)$ such that the brick vector $b(J)$ belongs to F . Define $J^F := \{j \in J : r(J, j) \in V_F\}$ as the subset of J consisting of indices whose corresponding roots lie in the affine vector space \tilde{V}_F , and

let $I = J \setminus J^F$. For any facet $J' \in \mathcal{SC}(Q, w)$, we have the following equivalence:

$$I \subseteq J' \quad \text{if and only if} \quad b(J') \in \tilde{V}_F.$$

Proof. \Rightarrow : Assume $I \subseteq J'$. Note that there exists a sequence of flips $J = J_0 \xrightarrow{j_0} J_1 \xrightarrow{j_1} \dots \xrightarrow{j_{\ell-1}} J_\ell = J'$ that never flips an element in I . This is due to the connectedness of the flip graph of a subword complex, especially for $\mathcal{SC}(Q_{[m] \setminus I}, w)$, where Q is of length m .

Now the following holds:

- 1) $r(J_k, j) \in V_F$ if $j \in J_k \setminus I$ (Case 1 and Case 2)
- 2) $r(J_k, i) \notin V_F$ if $i \in I$ (Case 3)

To prove this, it is enough to examine only one flip. Without loss of generality, take the first flip. Let $J_1 = J_0 \setminus \{j_0\} \cup \{j'_0\}$. Using Lemma 2.11, we proceed as follows:

Case 1: Let $i \in I$, then

$$r(J_1, i) = \begin{cases} s_\beta(r(J_0, i)) & \text{if } \min(i, j_0) < k \leq \max(i, j_0) \\ r(J_0, i) & \text{otherwise} \end{cases}$$

for $\beta := r(J_0, j_0)$. Since $\beta \in V_F$ and $r(J_0, i) \notin V_F$ Observation 3.26 implies $r(J_1, i) \notin V_F$.

Case 2: Let $j \in J_0 \cap J_1$, then

$$r(J_1, j) = \begin{cases} s_\beta(r(J_0, j)) & \text{if } \min(j, j_0) < k \leq \max(j, j_0) \\ r(J_0, j) & \text{otherwise} \end{cases}$$

holds. By Observation 3.26 in either case $r(J_1, j) \in V_F$.

Case 3: Let $j = j'_0$, then

$$r(J_1, j'_0) = \begin{cases} s_\beta(r(J_0, j'_0)) & \text{if } \min(j_0, j'_0) < k \leq \max(j_0, j'_0) \\ r(J_0, j'_0) & \text{otherwise} \end{cases}$$

but $r(J_0, j'_0) = \pm r(J_0, j_0) \in V_F$, hence $r(J_1, j'_0) \in V_F$.

Therefore, 1) and 2) hold. Now, note that $b(J_1) = b(J_0) + c_{0,1}r(J_0, j_0)$, for some constant $c_{0,1}$. Since $r(J_0, j_0) \in V_F$, we have $b(J_1) \in \tilde{V}_F$. Applying the same argument several times yields $b(J_\ell) = b(J') \in \tilde{V}_F$.

\Leftarrow : Let $q = b(J') \in \tilde{V}_F$ and $b(J_{F,\min})$ be the minimal element by Lemma 3.25. We will show that J' can be connected to J_{\min} by a sequence of decreasing flips $J' = J'_0 \xrightarrow{j'_0} J'_1 \xrightarrow{j'_1} \dots \xrightarrow{j'_{\ell-1}} J'_\ell = J_{\min}$, with $r(J'_k, j'_k) \in V_F$ for all $1 \leq k < \ell'$. To demonstrate this, we provide a construction of a flip-sequence. Let $p_{\min} := b(J_{F,\min})$. By the local cone property (Theorem 2.21), $p_{\min} - q$ is equal to

$$\sum_{j' \in J'} a_{j'} r(J', j') = b(J_{F,\min}) - b(J') \in V_F,$$

where $a_{j'} \geq 0$ for all $j' \in J'$. Let η_F be a linear functional that is minimal at the face F . Taking the inner product with η_F , we obtain:

$$0 = \sum_{j' \in J'} a_{j'} \langle \mathbf{r}(J', j'), \eta_F \rangle$$

but $\langle \mathbf{r}(J', j'), \eta_F \rangle = 0$ if $\mathbf{r}(J', j') \in V_F$ and $\langle \mathbf{r}(J', j'), \eta_F \rangle > 0$ otherwise. So, $a_{j'} = 0$ if $\mathbf{r}(J', j') \notin V_F$. Therefore,

$$b(J_{F,\min}) - b(J) = \sum_{\substack{j' \in J' \\ \mathbf{r}(J', j') \in V_F}} a_{j'} \mathbf{r}(J', j').$$

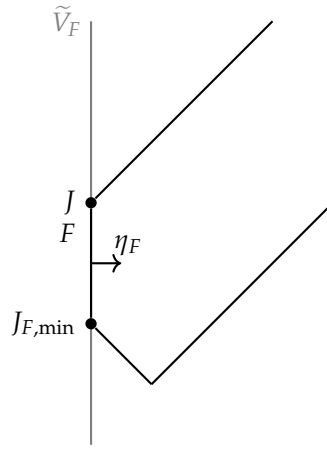


Figure 3.15: Normal vector η_F .

Since $J_{F,\min}$ minimizes the linear functional η , the inner product with η satisfies

$$\langle \eta, b(J_{F,\min}) - b(J) \rangle < 0.$$

If all $\mathbf{r}(J', j') \in R(J) \cap V_F$ were positive roots, by Remark 2.9, $\langle \eta, b(J_{F,\min}) - b(J) \rangle > 0$ would hold. Thus, at least one $\mathbf{r}(J', j')$ must be a negative root, $\mathbf{r}(J', j') \in \Phi^- \cap V_F$. We then perform a decreasing flip along j' to obtain J'_1 and repeat this process until reaching the minimal element of the face. Therefore, we can find a sequence $J' \xrightarrow{j'_0} J'_1 \xrightarrow{j'_1} \dots \xrightarrow{j'_{\ell-1}} J_{F,\min}$ such that $\mathbf{r}(J'_k, j'_k) \in V_F$ for $1 \leq k < \ell$. Similarly, going through $J_{F,\min}$, we can find a sequence $J = J_1 \xrightarrow{j_0} J_1 \xrightarrow{j_1} \dots \xrightarrow{j_{\ell-1}} J_\ell = J'$ such that $\mathbf{r}(J_k, j_k) \in V_F$ for $1 \leq k < \ell$. By properties 1) and 2), we are never flipping an element in I such that $j_k \notin I$. Therefore, $I \subseteq J$ holds. Note that since $\mathbf{r}(J', j') \in \Phi^-$, then $j' \in J'$ is indeed a flippable element. □

3.4.1.3 Proof of Theorem 3.23

Theorem 3.23 follows from the following Proposition. Compare with [JS23, Proposition 4.6 and Remark 4.11].

Proposition. 3.29

Consider a face F of the brick polyhedron $\mathcal{B}(Q, w)$, let $J \in \mathcal{SC}(Q, w)$ be a facet such that the brick vector $b(J) \in F$ and $J^F := \{j \in J : r(J, j) \in V_F\}$. Then, the following hold:

- 1) for $I = J \setminus J^F$, we have $F = \mathcal{B}^I(Q, w)$ and
- 2) for $J' \in \mathcal{SC}(Q, w)$ a facet, we have $I \subseteq J'$ if and only if $b(J') \in F$.

Proof. By Lemma 3.28, $I \subseteq J'$ if and only if $b(J') \in F$, so 2) follows. The vertices of F are then $b(J')$ for $I \subseteq J'$, and the local cone at $b(J')$ inside F is the intersection of the local cone of $b(J')$ in the brick polyhedron $\mathcal{B}(Q, w)$ with \tilde{V}_F . This is precisely the local cone at $b(J')$ in the modified brick polyhedron $\mathcal{B}^I(Q, w)$. Thus, $F = \mathcal{B}^I(Q, w)$. □

3.4.2 Some faces of ν -brick polyhedra

In this subsection, we will outline some conditions under which the modified brick polyhedron $\mathcal{B}^I(Q_\nu, w_\nu)$ is a face of the ν -brick polyhedron $\mathcal{B}(Q_\nu, w_\nu)$. The following notation will be used throughout our discussion.

Definition 3.30

For a ν -tree T we denote by β_t the root $\beta_t = r(T, t) = e_i - e_j$, for $t \in T$. We label the corresponding node $t \in T$ by ij for convenience and define the cone $C(T) := \{x \in V \mid \langle x, \beta_t \rangle > 0 \text{ for all } t \in T\}$. Given a subset of nodes $M \subseteq T$ we denote the ν -tree with M marked by T_M and define $C(T_M) := \{x \in V \mid \langle x, \beta_t \rangle > 0 \text{ for all } t \in T \setminus M \text{ and } \langle x, \beta_t \rangle = 0 \text{ for all } t \in M\}$. An example is shown in Figure 3.16.

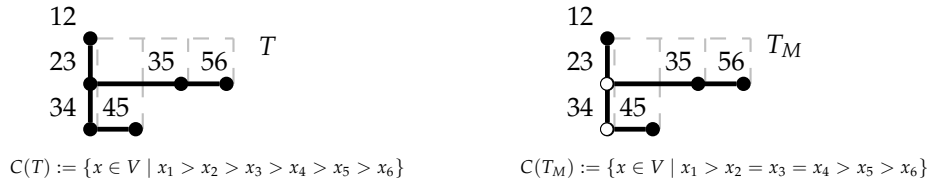


Figure 3.16: Left: ν -tree T , Right: ν -tree with marked points T_M .

Remark 3.31

The result [Ber+23, Theorem 4.17] asserts that all facets of the subword complex associated with the ν -Tamari lattice are acyclic. This condition is equivalent to the contact graph of the corresponding sorting network (or pipe dream) being acyclic, which in turn is equivalent to the system of inequalities having a solution. Therefore, the cone $C(T)$ is non-empty if and only if the corresponding contact graph is acyclic, a property that holds for ν -trees.

Lemma. 3.32

Let $I = T \setminus A$, where T is a ν -tree and $A \subseteq T$ a subset of ascents and define $\beta_t := r(T, t)$, $t \in T$.

There exists a linear functional f such that

$$f(\beta_a) = 0 \text{ for } a \in A \text{ and } f(\beta_t) > 0 \text{ for } t \in T \setminus A. \quad (3.1)$$

The proof idea of Lemma 3.32 relies on Definition 3.30 and is exemplified in Example 3.33.

Example 3.33

Consider $\nu = EEN$. All three ν -trees T, T' and T'' are shown in Figure 3.17.

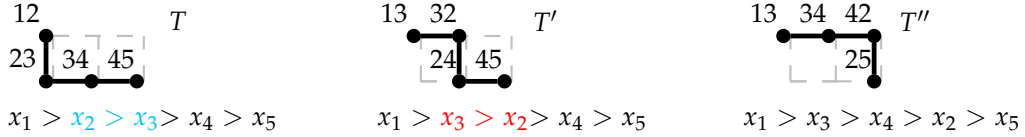


Figure 3.17: ν -trees for $\nu = EEN$ and defining inequalities for $C(T), C(T'), C(T'')$.

We are going to find a vector $f \in \mathbb{R}^5$ satisfying (3.1) for the ν -tree T and the only ascent marked, illustrated in Figure 3.19. Therefore, we need to solve $\langle f, e_2 - e_3 \rangle = 0$ and $\langle f, \beta \rangle > 0$ for $\beta \in \mathbb{R}(T) \setminus \{e_2 - e_3\}$. In particular, f must satisfy $x_1 > x_2 = x_3 > x_4 > x_5$. Rotating the only ascent in T gives us the ν -tree T' . Considering the cones $C(T)$ and $C(T')$, we observe that these cones are separated by $\{x \in \mathbb{R}^5 \mid x_1 > x_2 = x_3 > x_4 > x_5\}$, as illustrated schematically in Figure 3.18. A point $p \in C(T)$ satisfies $p_2 > p_3$, and respectively $p' \in C(T')$ satisfies $p'_3 > p'_2$, and both p and p' satisfy all constraints except $x_2 > x_3$, respectively $x_2 < x_3$. As illustrated in Figure 3.18, these two cones are separated by $C = \{x \in \mathbb{R}^5 \mid x_1 > x_2 = x_3 > x_4 > x_5\}$. Therefore, along the line segment connecting p and p' , there exists a point that satisfies $x_1 > x_2 = x_3 > x_4 > x_5$.

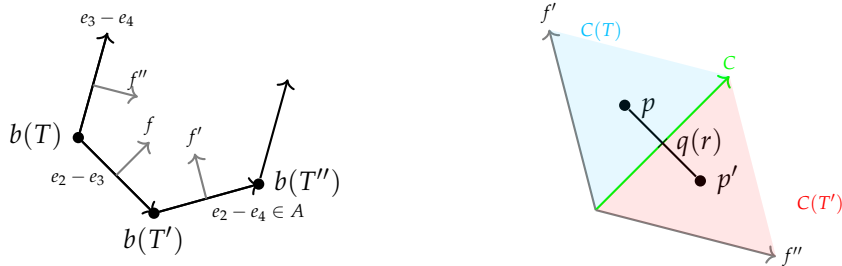


Figure 3.18: Left: Brick polyhedron for $\nu = EEN$, Right: Cones $C(T)$ and $C(T')$.

Firstly, define the cone \bar{D} as the set of points satisfying the inequalities defining both $C(T)$ and $C(T')$, but removing the inequalities $x_2 > x_3$ and $x_3 > x_2$. In symbols:

$$\bar{D} := \{x \in V \mid x_1 > x_2, x_3 > x_4 > x_5\}.$$

Since by definition $C(T) \subseteq \bar{D}$ and $C(T') \subseteq \bar{D}$ hold, we have for $p = (p_1, \dots, p_5) \in C(T)$ and $p' = (p'_1, \dots, p'_5) \in C(T')$, $p, p' \in \bar{D}$. Defining $q(t) := (1-t)p + tp'$ for $t \in [0, 1]$ gives us $q_2(0) = p_2 > p_3 = q_3(0)$ and $q_2(1) = p'_2 < p'_3 = q_3(1)$. Therefore, there exists $r \in [0, 1]$ such that $q_2(r) = q_3(r)$. Since all other inequalities of C hold, $f = q(r) \in C$ is a solution.

Proof.[Lemma 3.32] We proceed by induction on the number of marked ascents $k := |A|$. The statement holds for $k = 0$ by [Ber+23, Theorem 4.17], see Remark 3.31. Suppose $k \geq 1$ and that



Figure 3.19: Marked ν -trees T_M and $T'_{M'}$ for $\nu = EEN$.

the statement holds for $k - 1$. Let $I = T \setminus A$, where T is a ν -tree and $A \subseteq T$ is a subset of ascents with $|A| = k$, and let $\beta_t = r(T, t)$, $t \in T$ as above.

Let $\bar{a} \in A$ be the north-east most node in A (i.e. no other node in A is located north-east of \bar{a}), and let $T' = T \setminus \{\bar{a}\} \cup \{\bar{a}'\}$ be the ν -tree obtained from T by rotating \bar{a} . Let i_1, i_2, i_3, i_4 be the pipes

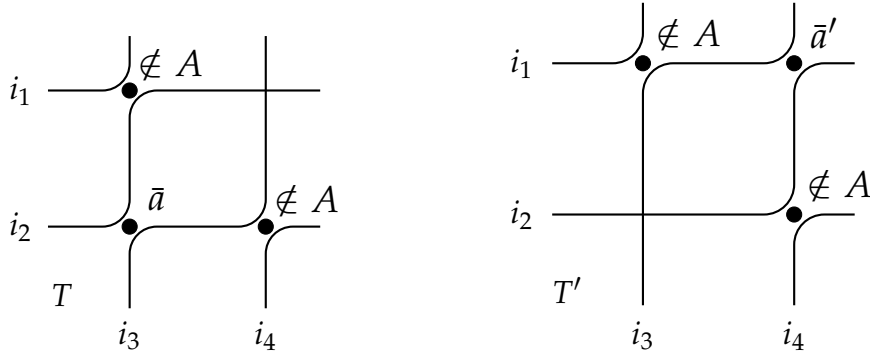


Figure 3.20: Structure of ν -trees T and T' .

passing through the nodes of T involved in the rotation of $\bar{a} \in T$, as illustrated in Figure 3.20. Let $\bar{A} = A \setminus \{\bar{a}\}$, then $\bar{A} \subseteq T$ is a subset of ascents of T with $|\bar{A}| = k - 1$ and $\bar{A} \subseteq T'$ is also a subset of ascents of T' . By induction hypothesis, the inequalities and equalities defining $C(T_{\bar{A}})$ and $C(T'_{\bar{A}})$ have solutions. Let

$$p = (p_1, \dots, p_\ell) \in C(T_{\bar{A}}),$$

$$p' = (p'_1, \dots, p'_\ell) \in C(T'_{\bar{A}}).$$

Note that all defining inequalities and equalities defining $C(T_{\bar{A}})$ and $C(T'_{\bar{A}})$ coincide, except for three:

$$x_{i_1} > x_{i_2} > x_{i_3} > x_{i_4} \text{ in } C(T_{\bar{A}}),$$

$$x_{i_1} > x_{i_3} > x_{i_2} > x_{i_4} \text{ in } C(T'_{\bar{A}}).$$

On the other hand, the defining inequalities and equalities for $C(T_A)$ are all other defining inequalities for $C(T_{\bar{A}})$ and $C(T'_{\bar{A}})$ together with

$$x_{i_1} > x_{i_2} = x_{i_3} > x_{i_4} \text{ in } C(T_A).$$

Let \bar{D} be defined by the other inequalities and equalities together with

$$x_{i_1} > x_{i_2}, x_{i_3} > x_{i_4}.$$

Note that we do not put any condition between x_{i_2} and x_{i_3} in \bar{D} , while

$$\begin{aligned} x_{i_2} &> x_{i_3} \text{ in } C(T_{\bar{A}}), \\ x_{i_3} &> x_{i_2} \text{ in } C(T'_{\bar{A}}), \\ x_{i_2} &= x_{i_3} \text{ in } C(T_A). \end{aligned}$$

We want to show that $C(T_A) \neq \emptyset$. For this, note that $C(T_{\bar{A}}) \subseteq \bar{D}$ and $C(T'_{\bar{A}}) \subseteq \bar{D}$. Therefore

$$q(t) = (1-t)p + tp' \in \bar{D} \text{ for all } t \in [0, 1].$$

Since

$$q_{i_2}(0) = p_{i_2} > p_{i_3} = q_{i_3}(0) \text{ and } q_{i_2}(1) = p'_{i_2} < p'_{i_3} = q_{i_3}(1).$$

Then, there must be some $r \in [0, 1]$ such that

$$q_{i_2}(r) = q_{i_3}(r).$$

Since all other defining inequalities of $C(T_A)$ are satisfied for $q(r)$, then

$$q(r) \in C(T_A).$$

Thus, $C(T_A)$ has a solution as wanted. □

Remark 3.34

Note that Lemma 3.32 is not necessarily true if $A \subseteq T$ is not a subset of ascents, as demonstrated in Example 3.35.

Example 3.35

Let us continue Example 3.21 and consider the marked ν -trees T_{M_2} , T_{M_3} , and T'_{M_4} as illustrated in Figure 3.21 and let $I_2 = T \setminus M_2$, $I_3 = T \setminus M_3$, $I_4 = T' \setminus M_4$.

For T_{M_2} , we obtain the conditions $x_1 > x_2 = x_3 = x_4 > x_5 > x_6$, which has a solution, and the modified brick polyhedron $\mathcal{B}^{I_2}(Q_\nu, w_\nu)$ is a face. For T_{M_3} , we obtain the conditions $x_1 > x_2 > x_3 > x_4 = x_5 > x_6$ with $x_3 = x_5$, which has no solution, and the modified brick polyhedron $\mathcal{B}^{I_3}(Q_\nu, w_\nu)$ is not a face. For T'_{M_4} , we obtain the conditions $x_1 > x_3 = x_4 = x_5$ and $x_3 > x_2 > x_5 > x_6$, which has no solution, and the modified brick polyhedron $\mathcal{B}^{I_4}(Q_\nu, w_\nu)$ is not a face.

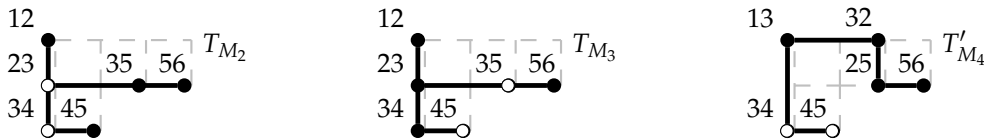


Figure 3.21: Marked ν -trees for $\nu = ENEEN$.

If we only replace inequalities by equalities for nodes corresponding to ascents, then there a solution and the modified brick polyhedron is face of the brick polyhedron:

Proposition. 3.36

Let $I = T \setminus A$, where T is a ν -tree and $A \subseteq T$ a subset of ascents. Then the modified brick polyhedron $\mathcal{B}^I(Q_\nu, w_\nu)$ is a face of the ν -brick polyhedron $\mathcal{B}(Q_\nu, w_\nu)$.

Proof. Take f as in Lemma 3.32 and let F be the face of the brick polyhedron $\mathcal{B}(Q_\nu, w_\nu)$ minimizing f . Since for every ν -tree \tilde{T} we have

$$b(\tilde{T}) - b(T) = \sum_{t \in T} c_t \mathbf{r}(T, t) \text{ for some } c_t \geq 0.$$

Then $f(b(\tilde{T})) \geq f(b(T))$, with equality satisfied when $b(\tilde{T}) - b(T) \in V_F$, the vector space spanned by $\{\mathbf{r}(T, a) \mid a \in A\}$. In particular $b(T) \in F$ and by Proposition 3.29 2)

$$b(\tilde{T}) \in F \iff T \setminus A = I \subseteq \tilde{T}.$$

Now $F = \mathcal{B}(Q_\nu, w_\nu) \cap \widetilde{V}_F$, and the local cone at point $b(\tilde{T})$ inside F is the intersection of the local cone of $b(\tilde{T})$ in $\mathcal{B}(Q_\nu, w_\nu)$ with \widetilde{V}_F . This is equal to the local cone of $b(\tilde{T})$ in $\mathcal{B}^I(Q_\nu, w_\nu)$. Therefore, $F = \mathcal{B}^I(Q_\nu, w_\nu)$. □

3.4.3 Bounded faces of ν -brick polyhedra

The goal of this section is to show that the faces in Proposition 3.36 are exactly the bounded faces of the ν -brick polyhedron (Corollary 3.45 and Corollary 3.47).

3.4.3.1 The spherical and root independent property

We denote by $Q_{\nu, I}$ the word obtained from Q_ν by deleting the letters with positions in I , and consider the corresponding subword complex $\mathcal{SC}(Q_{\nu, I}, w_\nu)$. Note that $\mathcal{SC}(Q_{\nu, I}, w_\nu) \neq \mathcal{SC}^I(Q_\nu, w_\nu)$, since every element in $\mathcal{SC}^I(Q_\nu, w_\nu)$ is of the form $I \cup J$ for $J \in \mathcal{SC}(Q_{\nu, I}, w_\nu)$. The purpose of this section is to show that $\mathcal{SC}(Q_{\nu, I}, w_\nu)$ is spherical and root independent. As a consequence, $\mathcal{SC}(Q_{\nu, I}, w_\nu)$ is realized as the polar of the brick polytope $\mathcal{B}(Q_{\nu, I}, w_\nu)$, which is combinatorially isomorphic to $\mathcal{B}^I(Q_\nu, w_\nu)$. Before doing this, we need some preliminaries.

Theorem 3.37: [PS15]

If $\mathcal{SC}(Q, w_\circ)$ is root independent, then it is realized by the polar of the brick polytope $\mathcal{B}(Q, w_\circ)$.

Lemma. 3.38: [Ces22], [CLS14]

Every spherical subword complex $\mathcal{SC}(Q, w)$ is isomorphic to a (spherical) subword complex of the form $\mathcal{SC}(\tilde{Q}, w_\circ)$.

Remark 3.39: Completing

For any spherical subword complex $\mathcal{SC}(Q, w)$, there exists a word w' , such that $ww' = w_\circ$ with $\ell(w) + \ell(w') = \ell(w_\circ)$, by completing w to w_\circ . By defining $Q' = Qw'$, the subword complexes $\mathcal{SC}(Q, w)$ and $\mathcal{SC}(Q', w_\circ)$ are isomorphic and the brick polytope $\mathcal{B}(Q, w)$ is just a translation

of $\mathcal{B}(Q', w_\circ)$.

The following result is assumed/mentioned in [PS15] but not explicitly written down. We include it here with proof for completeness.

Corollary 3.40

Every spherical, root independent subword complex $\mathcal{SC}(Q, w)$, where w is not necessary equal to w_\circ , is realized by the polar of the brick polytope $\mathcal{B}(Q, w)$.

Proof. By Lemma 3.38, $\mathcal{SC}(Q, w) \cong \mathcal{SC}(Q', w_\circ)$ by completing, as in Remark 3.39 the facets and root configurations do not change, so $\mathcal{SC}(Q', w_\circ)$ is root independent and we can apply Theorem 3.37. Moreover the brick polytope of $\mathcal{SC}(Q', w_\circ)$ is a translation of the brick polytope of $\mathcal{SC}(Q, w)$, so the Corollary holds. □

Now, our goal is to show that $\mathcal{SC}(Q_{\nu, I}, w_\nu)$ is spherical and root independent for interior faces I .

Lemma. 3.41: Spherical

For an interior face $I \in \mathcal{SC}(Q_\nu, w_\nu)$, the subword complex $\mathcal{SC}(Q_\nu^I, w_\nu)$ is realizable as the boundary of a polytope, hence it is spherical.

Proof. If I is an interior face then the set of faces $\{J \in \mathcal{SC}(Q_\nu, w_\nu) : I \subseteq J\}$, ordered by reverse containment is the face poset of the face of the ν -associahedron corresponding to I . But the reverse containment poset on $\{J \in \mathcal{SC}(Q_\nu, w_\nu) : I \subseteq J\}$ is isomorphic to the reverse cotainment poset faces of $\mathcal{SC}(Q_{\nu, I}, w_\nu)$. And by [CPS19, Proposition 5.16] the cells of the ν -associahedron are known to be products of classical associahedra, in particular they are polytopes. And $\mathcal{SC}(Q_{\nu, I}, w_\nu)$ can be realized as the boundary complex of the polar of the polytope of the corresponding cell. Hence $\mathcal{SC}(Q_{\nu, I}, w_\nu)$ is polytopal, hence spherical. □

Remark 3.42

Observe, a single pipeline cannot have more than two turns inside the Ferrer's diagram F_ν . Otherwise, there would exist at least three vertices, as shown in Figure 3.22 (Left) in the ν -tree, but then the two red points would be ν -incompatible, which contradicts the definition of a ν -tree as a maximal set of ν -compatible elements.

Lemma. 3.43: Root Independent

Let I be an interior face of $\mathcal{SC}(Q_\nu, w_\nu)$, T a ν -tree and $A \subseteq T$ a subset of ascents of T such that $I = T \setminus A$.

- 1) $\{r(T, a) : a \in A\}$ is linearly independent.
- 2) $\mathcal{SC}(Q_{\nu, I}, w_\nu)$ is root independent.

Proof.

To show 1), we proceed by induction on $n = |A|$. The statement is clear for $n = 1$. Suppose that $n \geq 2$ and that the statement holds for $n - 1$.

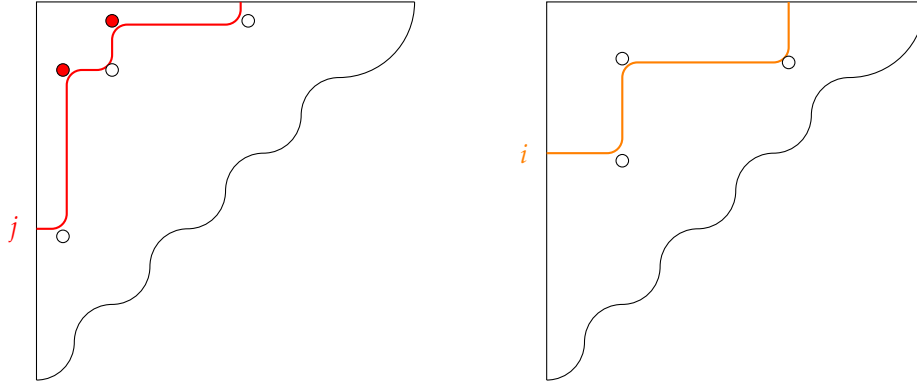


Figure 3.22: Left: A pseudoline with 3 turns exhibiting red vertices in ν -incompatible position, Right: A pseudoline with 2 turns showing all vertices in ν -compatible position.

Let $a_2 \in A$ such that $r(T, a_2) = e_i - e_j$ with the smallest possible i . Since $a_2 \in A$ is an ascent, there is a node to the North and one to the East. By Remark 3.42, there cannot be a node to the left of a_2 , as illustrated in Figure 3.23 (Right). Furthermore, since i is chosen to be minimal, a_2 is unique. Additionally, there can be no vertex on the line segment between the vertices a_2 and a_3 , following the same argument.

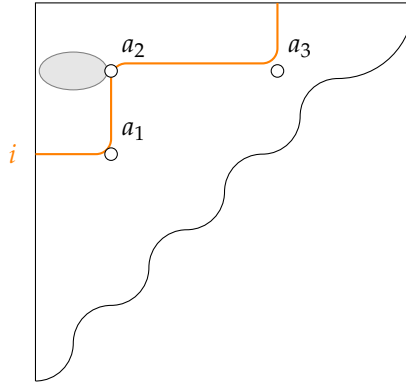


Figure 3.23: No node in gray area.

Now, suppose there exists a linear combination such that $\sum_{a \in A} c_a r_I(a) = 0$. Since $r_I(a_2) = e_i - e_j$ with i being minimal, there is no summand of the form $e_k - e_i$, hence $c_{a_2} = 0$. Therefore $\sum c_a r_I(a)$ is a sum of $n - 1$ summands and by induction hypothesis, we obtain $c_a = 0$ for all $a \in A$. So 1) follows.

To prove 2) it is enough to find a facet of $\mathcal{SC}(Q_{\nu, I}, w_\nu)$ whose root configuration is linearly independent. Taking the facet $A \subseteq \mathcal{SC}(Q_{\nu, I}, w_\nu)$ and applying 1) conclude 2). □

Corollary 3.44

The subword complex $\mathcal{SC}(Q_{\nu, I}, w_\nu)$ is realized by the polar of the brick polytope $\mathcal{B}(Q_{\nu, I}, w_\nu)$. In particular $\mathcal{B}(Q_{\nu, I}, w_\nu)$ is a bounded polytope.

Proof. By Lemma 3.41 and Lemma 3.43, $\mathcal{SC}(Q_{\nu, I}, w_\nu)$ is spherical and root independent. Therefore, it is realized by the polar of $\mathcal{B}(Q_{\nu, I}, w_\nu)$ by Corollary 3.40. □

Corollary 3.45

Let T a ν -tree, $A \subseteq T$ be a subset of ascents, and $I = T \setminus A$ be the corresponding interior face of $\mathcal{SC}(Q_\nu, w_\nu)$. Then, $\mathcal{B}^I(Q_\nu, w_\nu)$ is a bounded face of the ν -brick polyhedron. Moreover,

$$\mathcal{B}^I(Q_\nu, w_\nu) = \text{conv}\{b(J) \mid I \subseteq J \text{ a facet of } \mathcal{SC}(Q_\nu, w_\nu)\}$$

and its face poset is the reverse containment poset on the set $\{J \in \mathcal{SC}(Q_\nu, w_\nu) : I \subseteq J\}$.

Proof. By [JS23, Remark 4.11] the brick polytope $\mathcal{B}(Q_{\nu,I}, w_\nu)$ and the brick polyhedron $\mathcal{B}^I(Q_\nu, w_\nu)$ share the following properties:

- 1) Their vertices are in correspondence ($J \in \mathcal{SC}(Q_{\nu,I}, w_\nu) \iff I \cup J \in \mathcal{SC}^I(Q_\nu, w_\nu)$).
- 2) Their edge directions are the same, although they may have different lengths (roots in the root configuration and modified root configuration are the same).
- 3) Their local cones at the vertices are the same.

In particular, $\mathcal{B}(Q_{\nu,I}, w_\nu)$ and $\mathcal{B}^I(Q_\nu, w_\nu)$ are combinatorially isomorphic, and in particular bounded (Corollary 3.44). Since $\mathcal{SC}(Q_{\nu,I}, w_\nu)$ is realized by the polar of $\mathcal{B}(Q_{\nu,I}, w_\nu)$ by Corollary 3.44, transforming the facets $J \in \mathcal{SC}(Q_{\nu,I}, w_\nu)$ to facets $I \cup J \in \mathcal{SC}^I(Q_\nu, w_\nu)$ we obtain:

$$\mathcal{B}^I(Q_\nu, w_\nu) = \text{conv}\{b(J) \mid I \subseteq J \text{ a facet of } \mathcal{SC}(Q_\nu, w_\nu)\}.$$

Also, since the face poset of $\mathcal{B}(Q_{\nu,I}, w_\nu)$ is the reverse containing poset of faces $J \in \mathcal{SC}(Q_{\nu,I}, w_\nu)$, then adding I to each face we obtain that the face poset of $\mathcal{B}^I(Q_\nu, w_\nu)$ is the reverse containment poset on the set $\{J' \in \mathcal{SC}(Q_\nu, w_\nu) \mid I \subseteq J'\}$ as desired. □

3.4.3.2 Unique representation of bounded faces**Lemma. 3.46**

Let T be a ν -tree, $A \subseteq T$ a subset of ascents, $I = T \setminus A$ and $F = \mathcal{B}^I(Q_\nu, w_\nu)$ be the corresponding bounded face of the ν -brick polyhedron $\mathcal{B}(Q_\nu, w_\nu)$. Then

- 1) $T = J_{F,\min}$ and $A = J_{F,\min}^F$.
- 2) If $F = \mathcal{B}^{I'}(Q_\nu, w_\nu)$ for $I' = T' \setminus A'$ where T' is a ν -tree and $A' \subseteq T'$ a subset of ascents, then $T = T'$, $A = A'$ and $I = I'$.

Proof. 1) $J_{F,\min}$ is the unique facet $I \subseteq J$ such that $j \in J \setminus I$ is increasingly flippable. Since T satisfies this property, then $T = J_{F,\min}$. Moreover, $J_{F,\min}^F = J_{F,\min} \setminus I = T \setminus A$.

2) follows from 1). □

Corollary 3.47

The bounded faces of the ν -brick polyhedron $\mathcal{B}(Q_\nu, w_\nu)$ are exactly, the $\mathcal{B}^I(Q_\nu, w_\nu)$, for $I = T \setminus A$, T a ν -tree and $A \subseteq T$ a subset of ascents.

Proof. By Corollary 3.45, if T is a ν -tree, $A \subseteq T$ a subset of ascents, and $I = T \setminus A$ then $\mathcal{B}^I(Q_\nu, w_\nu)$ is a bounded face of $\mathcal{B}(Q_\nu, w_\nu)$. Now let F be a bounded face of $\mathcal{B}(Q_\nu, w_\nu)$. Now let F be a bounded face of $\mathcal{B}(Q_\nu, w_\nu)$, $T = J_{F, \min}$ and $A = J_{F, \min}^c$. Since F is bounded then every element of A is flippable in T , otherwise F would contain an infinite ray. Moreover, every $a \in A$ is increasingly flippable in T , because T is the minimal element of the face. The face $F = \mathcal{B}^I(Q_\nu, w_\nu)$ as desired. \square

Question 3.48

Can we characterize the sets I for which $\mathcal{B}^I(Q_\nu, w_\nu)$ is a face of $\mathcal{B}(Q_\nu, w_\nu)$? Corollary 3.47 gives an answer for bounded faces but we do not know an answer in general. See Example 3.21.

3.4.4 The poset of bounded faces of ν -brick polyhedra

In this section, we will demonstrate that the poset of bounded faces of the ν -brick polyhedron is anti-isomorphic to the poset of interior faces of the ν -subword complex, as stated in Theorem 3.18.

Proof.[Theorem 3.18] By Corollary 3.47, the bounded faces of $\mathcal{B}(Q_\nu, w_\nu)$ are exactly the $\mathcal{B}^I(Q_\nu, w_\nu)$ for the interior face $I = T \setminus A$ for some ν -tree T and $A \subseteq T$ a subset of ascents. We are going to show: If I_1, I_2 are interior faces of $\mathcal{SC}(Q_\nu, w_\nu)$ then

$$I_1 \subseteq I_2 \iff \mathcal{B}(Q_{\nu, I_1}, w_\nu) \supseteq \mathcal{B}(Q_{\nu, I_2}, w_\nu).$$

Corollary 3.45 implies that if I is an interior face, then

$$\mathcal{B}^I(Q_\nu, w_\nu) = \text{conv}\{b(J) \mid I \subseteq J \text{ facet}\}.$$

Therefore, if $I_1 \subseteq I_2$ then $\mathcal{B}^{I_2}(Q_\nu, w_\nu) \subseteq \mathcal{B}^{I_1}(Q_\nu, w_\nu)$. Indeed all faces of $\mathcal{B}^{I_1}(Q_\nu, w_\nu)$ are of the form $\mathcal{B}^J(Q_\nu, w_\nu)$ for $I_1 \subseteq J$.

We are labelling faces of the brick polyhedron by $\mathcal{B}^J(Q_\nu, w_\nu)$, where $J = T \setminus A$, such a labelling is unique by Lemma 3.46. Now take a face $\mathcal{B}^{I_2}(Q_\nu, w_\nu)$ of $\mathcal{B}^{I_1}(Q_\nu, w_\nu)$ then $\mathcal{B}^{I_2}(Q_\nu, w_\nu) = \mathcal{B}^J(Q_\nu, w_\nu)$ for some $I_1 \subseteq J$. By uniqueness $I_2 = J \Rightarrow I_1 \subseteq I_2$. \square

Corollary 3.49

The complex of bounded faces of the ν -brick polyhedron is a realization of the ν -associahedron.

3.5 A projection of brick polyhedra

In this section, we investigate projections of brick polyhedra. Our focus includes providing a proof for the special case where ν has no two consecutive North steps, and we illustrate the gen-

eral case through two examples. Throughout this section, we use the notation $[N] := \{1, \dots, N\}$ for $N \in \mathbb{N}$.

3.5.1 The maximal polytopal part

Since the dimension of the ν -brick polyhedron can be higher than the dimension of the maximal polytopal part, we apply a projection π . To begin our study, we focus on understanding the dimension of the maximal polytopal part.

Definition 3.50: Maximal Polytopal Part of the ν -Brick Polyhedron

The dimension of the maximal polytopal part of the ν -brick polyhedron is given by the size of the the biggest stair case weakly above ν . In particular, the dimension d of the maximal polytopal part is:

$$d := \max\{\#\text{ valleys}(u) \mid u \text{ is a path weakly above } \nu \text{ inside } F_\nu\}.$$

For a path ν of length n , we associate coordinates to all lattice points in the Ferrers diagram F_ν by giving the top-left point the coordinate $(0, 0)$. Moving one step to the right (respectively down) increases the first (respectively second) coordinate by one. This is illustrated in Figure 3.25. For each point $p = (p_1, p_2) \in A_\nu$, we define $\chi(p) := p_1 + p_2$ and the k -th diagonal level $M_k = \{p \in A_\nu : \chi(p) = k\}$ for all $1 \leq k \leq n$.

Definition 3.51

For a finite path ν , with associated network \mathcal{N}_ν having N levels, let T be the ν -tree corresponding to the anti-greedy facet. We label the levels from top to bottom by $0, 1, \dots, N-1$ and denote the corresponding vertex in the ν -brick polyhedron by $x = b(T) = (x_0, \dots, x_{N-1})$. Since x_0 and x_{N-1} are constant for every ν -tree, we omit them and write just $x = b(T) = (x_1, \dots, x_{N-2})$. Since the sum of the coordinates is constant, then $\dim \mathcal{B}(Q_\nu, w_\nu) = N-3$. Let $\Sigma \subseteq [N]$ such that M_k for $k \in \Sigma$ represent the diagonal levels where nodes $t_1, \dots, t_\ell \in T$ exist between consecutive East or North steps. Let $S \subseteq \Sigma$ be a subset containing exactly one node of each diagonal level M_k for $k \in \Sigma$.

Define $\Gamma_\nu := \{r(T, t) \mid t \in S\} \subseteq \mathcal{E}^+(w_\nu, \text{Dem}(Q_\nu))$. Since $t \in S$ is non-flippable in T then $r(T, t) \in \mathcal{E}^+(w_\nu, \text{Dem}(Q_\nu))$. Moreover, denote the cardinality of Γ_ν by $\gamma := |\Gamma_\nu|$. An example where Γ_ν is unique is shown in Figure 3.24. Moreover, Γ_ν implies a partition of $[N]$ by grouping all indices i, j that appear in some element $e_i - e_j \in \Gamma_\nu$.

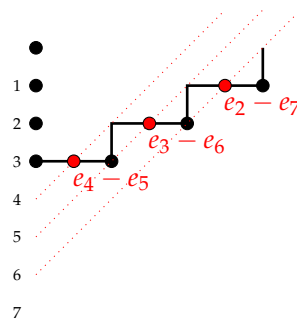


Figure 3.24: Γ_ν for $\nu = EENEENEEN$ with partition $\{1\}, \{2, 7\}, \{3, 6\}, \{4, 5\}, \{8\}$.

Lemma. 3.52

The dimension of the maximal polytopal part d of the ν -brick polyhedron is given by

$$d = N - 3 - \gamma, \tag{3.2}$$

where N is the number of levels of \mathcal{N}_ν , and γ is the number of lines through two consecutive East or North steps.

Proof. This is easily seen in Figure 3.25. The number of diagonal levels going through the interior of at least one box in F_ν is $N - 3$. We find the largest stair case weakly above ν by increasing it from $(0,0)$ until we touch ν . From this point, we subtract the number of diagonal levels, getting $d = N - 3 - \gamma$.

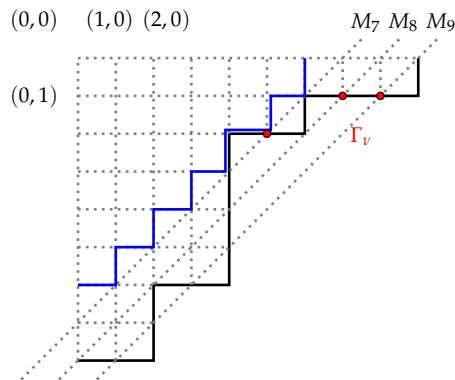


Figure 3.25: Biggest stair case (blue) and a choice of nodes for Γ_ν (red).

□

Example 3.53

For $\nu = EEENNN$, we have $N = 8$ levels and $|\Gamma_\nu| = \gamma = 2$. By Lemma 3.52, we obtain $d = N - 3 - \gamma = 8 - 3 - 2 = 3$. In Figure 3.26, we see a clear comparison of the relevant points for counting $N - 3$, and the cardinality of Γ_ν .



Figure 3.26: Relevant points for Left: $N - 3$, Right: Γ_ν for $\nu = EEENNN$.

3.5.2 A projection in a special case

In this subsection, we consider the special case where ν has no two consecutive North steps. This assumption allows us to offer a nice projection. We will denote the dimension of the maximal polytopal part as d and the number of levels of \mathcal{N}_ν as N . As mentioned above we take $x = b(T) =$

(x_1, \dots, x_{N-2}) by omitting the first and last coordinates x_0 and x_{N-1} (which are constant). The set S in this case consists of all the points between two consecutive East steps in ν .

Remark 3.54

We denote the sum of the coordinates indexed by $i \in I$ as x_I . In particular, we denote the sum of coordinates $x_{i_k}, 1 \leq k \leq j$, as x_{i_1, \dots, i_j} .

Definition 3.55: Grouping

Let M_i for all $i = 1, \dots, d + 1$, be the partition of coordinates given by Γ_ν . For this case, we have $M_i = \{i\}$ union the diagonal levels plus 1 of $s \in S$ that are in the $i - 1$ horizontal line from top to bottom. We define the projection $\pi_1 : \mathbb{R}^{N-2} \rightarrow \mathbb{R}^{d+1}$, by sending each element $x = (x_1, \dots, x_{N-2}) \in \mathbb{R}^{N-2}$ to $(x_{M_1}, \dots, x_{M_d})$.

Definition 3.56: Projection

Since the sum of all brick vectors is constant, we apply a second projection $\pi_2 : \mathbb{R}^{d+1} \rightarrow \mathbb{R}^d$, defined as $(x_{M_1}, \dots, x_{M_{d+1}}) \mapsto (y_1, \dots, y_d) = (x_{M_1}, x_{M_1} + x_{M_2}, \dots, x_{M_1} + \dots + x_{M_d})$. We define $\pi : \mathbb{R}^{N-2} \rightarrow \mathbb{R}^d$ as $\pi = \pi_2 \circ \pi_1$.

Example 3.57

For $\nu = \text{EENEENEEN}$, we have $N - 2 = 7$ and $\Gamma_\nu = \{e_4 - e_5, e_3 - e_6, e_2 - e_7\}$, as illustrated in Figure 3.27. Then $M_1 = \{1\}$, $M_2 = \{2, 7\}$, $M_3 = \{3, 6\}$ and $M_4 = \{4, 5\}$.

$$\begin{aligned} (x_1, x_2, x_3, x_4, x_5, x_6, x_7) &\xrightarrow{\pi_1} (x_1, x_2 + x_7, x_3 + x_6, x_4 + x_5) \\ &\xrightarrow{\pi_2} (x_1, x_1 + x_2 + x_7, x_1 + x_2 + x_3 + x_6 + x_7) \\ &= (x_1, x_{1,2,7}, x_{1,2,3,6,7}) \end{aligned}$$

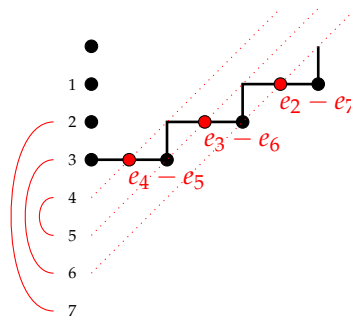


Figure 3.27: Coordinate grouping for projection (special case) for $\nu = \text{EENEENEEN}$.

Lemma. 3.58

If ν has no two consecutive North steps the first y_k in which x_i appears is y_i for all $1 \leq i \leq d$. Moreover x_i appears in y_i, y_{i+1}, \dots, y_d .

Proof. By the definition of π_1 , and since $i \in M_i$, it follows that x_i appears for the first time in y_i , and appears in all y_i afterwards. □

Lemma. 3.59: Projection Special Case

In the case where ν has no two consecutive North steps, the projection π of the ν -brick polyhedron $\mathcal{B}(Q_\nu, w_\nu)$ realizes the ν -associahedron. Moreover, this realization coincides with the canonical realization of the ν -associahedron up to translation.

Proof. Observe that the dimension of the maximal polytopal part and the projected points align precisely. Let T be a ν -tree and $T' = T \setminus \{b\} \cup \{b'\}$ be a rotation as in Figure 3.28.

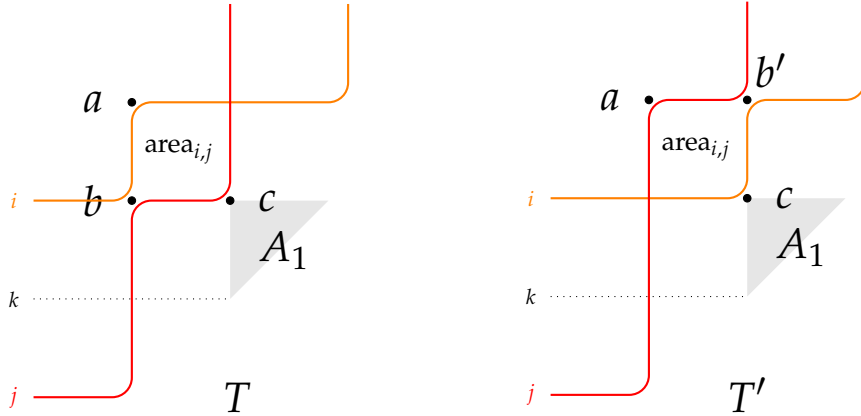


Figure 3.28: Structure of ν -trees T and T' .

Let $c(T) = (c_1, \dots, c_d)$ and $c(T') = (c'_1, \dots, c'_d)$ be the coordinates of the ν -trees T and T' in the canonical realization. We need to show

$$c(T) - c(T') = \pi(b(T')) - \pi(b(T)).$$

The translation vector from the canonical realization to the projection is then $\pi(b(T_0))$, where T_0 is the minimal ν -tree. Suppose that node $b \in T$ touches pseudolines i and j , and let k be the lower horizontal level of a descendant node of b in the tree T , see Figure 3.28. In the canonical realization, we have

$$c'_\ell = \begin{cases} c_\ell + \text{area}_{i,j} & \text{for } i \leq \ell \leq k \\ c_\ell & \text{otherwise} \end{cases}.$$

We need to show that this formula holds for the projected points. Let

$$\begin{aligned} y &= (y_1, \dots, y_d) = \pi(b(T)), \quad y' = (y'_1, \dots, y'_d) = \pi(b(T')), \\ x &= (x_1, \dots, x_{N-2}) = b(T), \quad x' = (x'_1, \dots, x'_{N-2}) = b(T'). \end{aligned}$$

Then $x'_i = x_i + \text{area}_{i,j}$, $x'_j = x_j - \text{area}_{i,j}$ and $x'_\ell = x_\ell$ otherwise. This is because in the ν -brick polyhedron x_i is minus the number of bricks below pseudoline i . When we make the flip/rotation, this number of bricks is reduced by $\text{area}_{i,j}$. Similarly, the number of bricks below pseudoline j increases by $\text{area}_{i,j}$. The number of bricks below and other pseudolines remains constant.

Now it is not hard to see that $j \in M_{k+1}$. If there is a node below b in T then $j = k + 1 \in M_{k+1}$, if not then j is the diagonal level plus 1 of the point $s \in S$ that is in the same column as b and in the

k -th horizontal line, so $j \in M_{k+1}$. Therefore, since

$$y_\ell = (x_{M_1} + \dots + x_{M_\ell}) \text{ and } y'_\ell = (x'_{M_1} + \dots + x'_{M_\ell})$$

then

$$y'_\ell = \begin{cases} y_\ell + \text{area}_{i,j} & \text{for } i \leq \ell \leq k \\ y_\ell & \text{otherwise} \end{cases}.$$

This finishes the proof. □

Example 3.60

Consider the path $\nu = EENEEN$ and use the labeling shown in Figure 3.29.

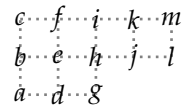


Figure 3.29: Grid for labeling of $SC(Q_\nu, w_\nu)$ for $\nu = EENEEN$.

We obtain the ν -Tamari lattice and rotation lattice shown in Figure 3.30. Here is a list of all facets:

- $I_1 = \{a, b, c, d, g, j, l\}$ $I_2 = \{a, c, d, g, j, k, l\}$ $I_3 = \{a, c, d, g, k, l, m\}$ $I_4 = \{c, d, f, g, k, l, m\}$
- $I_5 = \{c, f, g, i, k, l, m\}$ $I_6 = \{b, c, d, e, g, j, l\}$ $I_7 = \{b, c, e, g, h, j, l\}$ $I_8 = \{c, e, f, g, h, j, l\}$
- $I_9 = \{c, f, g, h, i, j, l\}$ $I_{10} = \{c, f, g, i, j, k, l\}$ $I_{11} = \{c, d, e, f, g, j, l\}$ $I_{12} = \{c, d, f, g, j, k, l\}$

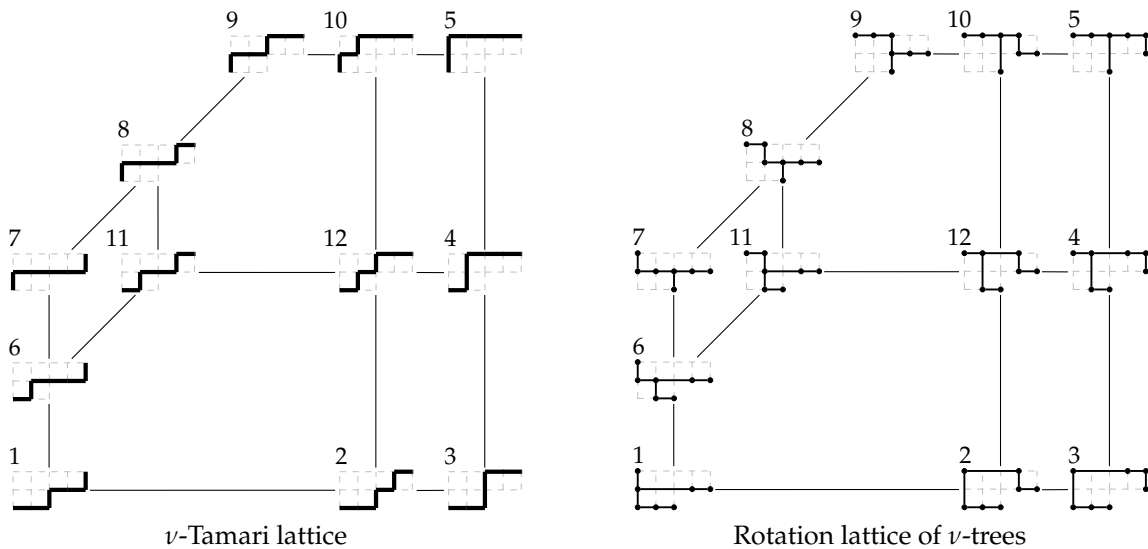


Figure 3.30: Example $\nu=EENEEN$.

The corresponding brick vectors (omitting the first and last coordinate, which are constant) are:

$$\begin{array}{lll}
B(I_1) = -(12, 8, 8, 5, 1)^\top & B(I_2) = -(9, 11, 8, 5, 1)^\top & B(I_3) = -(8, 11, 8, 5, 2)^\top \\
B(I_4) = -(8, 9, 10, 5, 2)^\top & B(I_5) = -(8, 7, 10, 7, 2)^\top & B(I_6) = -(12, 7, 9, 5, 1)^\top \\
B(I_7) = -(12, 6, 9, 6, 1)^\top & B(I_8) = -(11, 6, 10, 6, 1)^\top & B(I_9) = -(10, 6, 10, 7, 1)^\top \\
B(I_{10}) = -(9, 7, 10, 7, 1)^\top & B(I_{11}) = -(11, 7, 10, 5, 1)^\top & B(I_{12}) = -(9, 9, 10, 5, 1)^\top
\end{array}$$

By Lemma 3.52, the dimension of the maximal polytopal part is equal to $d = 2$. According to Definition 3.24, we obtain a unique $\Gamma_\nu = \text{cone}\{e_2 - e_5, e_3 - e_4\}$, as shown in Figure 3.31.

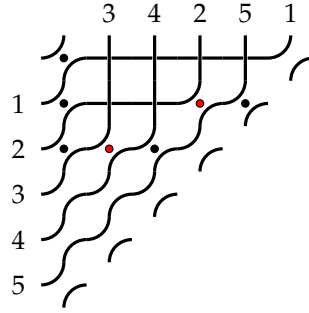


Figure 3.31: Pipe dream for anti-greedy facet for $\nu = EENEEN$ with $\Gamma_\nu = \{e_2 - e_5, e_3 - e_4\}$.

Applying π_1 to the brick vectors gives us the points:

$$\begin{array}{llll}
P'_1 = -(12, 9, 13)^\top & P'_2 = -(9, 12, 13)^\top & P'_3 = -(8, 13, 13)^\top & P'_4 = -(8, 11, 15)^\top \\
P'_5 = -(8, 9, 17)^\top & P'_6 = -(12, 8, 14)^\top & P'_7 = -(12, 7, 15)^\top & P'_8 = -(11, 7, 16)^\top \\
P'_9 = -(10, 7, 17)^\top & P'_{10} = -(9, 8, 17)^\top & P'_{11} = -(11, 8, 15)^\top & P'_{12} = -(9, 10, 15)^\top
\end{array}$$

Applying $\pi = \pi_2 \circ \pi_1$ to the brick vectors gives us the points:

$$\begin{array}{llll}
P_1 = -(12, 21)^\top & P_2 = -(9, 21)^\top & P_3 = -(8, 21)^\top & P_4 = -(8, 19)^\top \\
P_5 = -(8, 17)^\top & P_6 = -(12, 20)^\top & P_7 = -(12, 19)^\top & P_8 = -(11, 18)^\top \\
P_9 = -(10, 17)^\top & P_{10} = -(9, 17)^\top & P_{11} = -(11, 19)^\top & P_{12} = -(9, 19)^\top
\end{array}$$

The points from the canonical realization are the following:

$$\begin{array}{llll}
C_1 = (0, 0)^\top & C_2 = (3, 0)^\top & C_3 = (4, 0)^\top & C_4 = (4, 2)^\top \\
C_5 = (4, 4)^\top & C_6 = (0, 1)^\top & C_7 = (0, 2)^\top & C_8 = (1, 3)^\top \\
C_9 = (2, 4)^\top & C_{10} = (3, 4)^\top & C_{11} = (1, 2)^\top & C_{12} = (3, 2)^\top
\end{array}$$

In particular, we have the equality

$$C_i = P_i - P_1 \text{ for } 1 \leq i \leq 12,$$

as shown in Lemma 3.59.

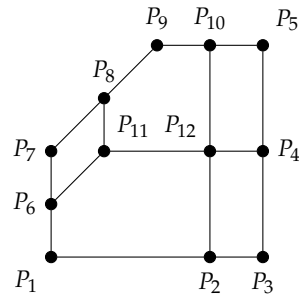


Figure 3.32: Projection of $\mathcal{B}(Q_\nu, w_\nu)$ for $\nu = EENEEN$.

3.5.3 A projection in the general case

In this chapter, we present two examples to illustrate the general case, although we do not provide a formal proof.

Example 3.61

Consider the path $\nu = EENN$ and use the labeling shown in Figure 3.33. By Lemma 3.52, the dimension of the maximal polytopal part is equal to $d = 2$. If we contract the whole Bruhat cone, we obtain a polytope of dimension 1, which is a contradiction to $d = 2$. Therefore, we have to choose exactly one element of the set $\{e_3 - e_4, e_1 - e_2\}$ for Γ_ν .

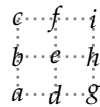


Figure 3.33: Grid for labeling of $SC(Q_\nu, w_\nu)$ for $\nu = EENEEN$.

Here is a list of all facets:

$$\begin{aligned} I_1 &= \{a, b, c, d, g\} & I_2 &= \{b, c, d, e, g\} & I_3 &= \{c, d, e, f, g\} \\ I_4 &= \{b, c, e, g, h\} & I_5 &= \{c, e, f, g, h\} & I_6 &= \{c, f, g, h, i\} \end{aligned}$$

The corresponding brick vectors are:

$$\begin{aligned} b(I_1) &= -(8, 5, 4, 1)^\top & b(I_2) &= -(8, 4, 5, 1)^\top & b(I_3) &= -(7, 4, 6, 1)^\top \\ b(I_4) &= -(8, 3, 5, 2)^\top & b(I_5) &= -(7, 3, 6, 2)^\top & b(I_6) &= -(6, 3, 6, 3)^\top \end{aligned}$$

We obtain the ν -Tamari lattice, rotation lattice and the bounded faces of the ν -brick polyhedron as shown in Figure 3.34.

For the canonical realization, we obtain the points C_i , $1 \leq i \leq 6$. See Figure 3.35 (Left).

$$\begin{aligned} C_1 &= (0, 0)^\top & C_2 &= (0, 1)^\top & C_3 &= (1, 2)^\top \\ C_4 &= (0, 2)^\top & C_5 &= (1, 3)^\top & C_6 &= (2, 4)^\top \end{aligned}$$

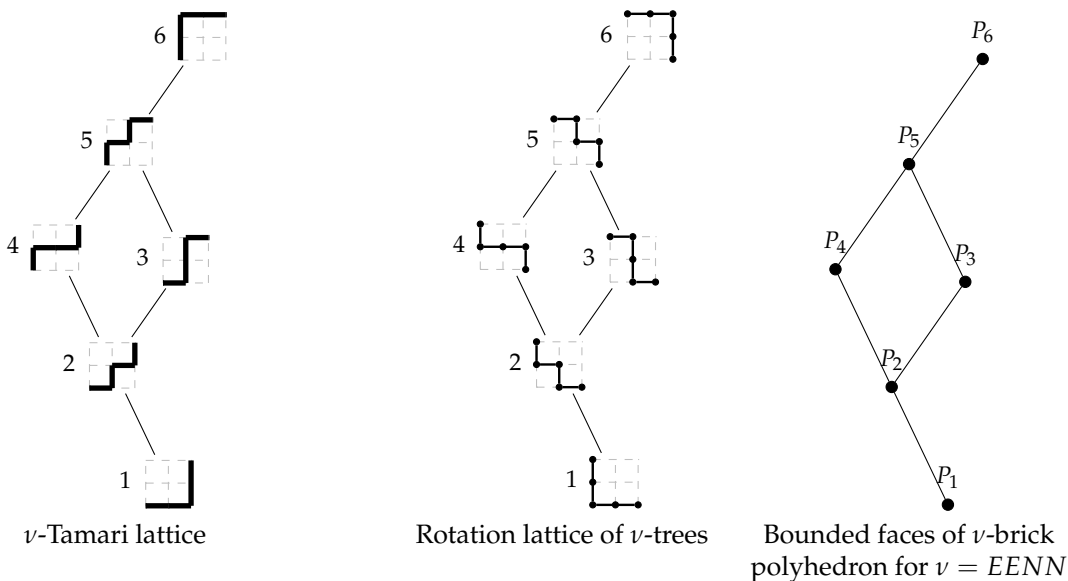


Figure 3.34: Example $\nu=EENN$.

For $\Gamma_\nu = \{e_1 - e_2\}$, we obtain projected points $P_i^{(1)}, 1 \leq i \leq 6$. See Figure 3.35 (Middle).

$$\begin{array}{lll}
 P_1^{(1)} = -(13, 17)^\top & P_2^{(1)} = -(12, 17)^\top & P_3^{(1)} = -(11, 17)^\top \\
 P_4^{(1)} = -(11, 16)^\top & P_5^{(1)} = -(10, 16)^\top & P_6^{(1)} = -(9, 15)^\top
 \end{array}$$

For $\Gamma_\nu = \{e_3 - e_4\}$, we obtain projected points $P_i^{(2)}, 1 \leq i \leq 6$. See Figure 3.35 (Right).

$$\begin{array}{lll}
 P_1^{(2)} = -(8, 13)^\top & P_2^{(2)} = -(8, 12)^\top & P_3^{(2)} = -(7, 11)^\top \\
 P_4^{(2)} = -(8, 11)^\top & P_5^{(2)} = -(7, 10)^\top & P_6^{(2)} = -(6, 9)^\top
 \end{array}$$

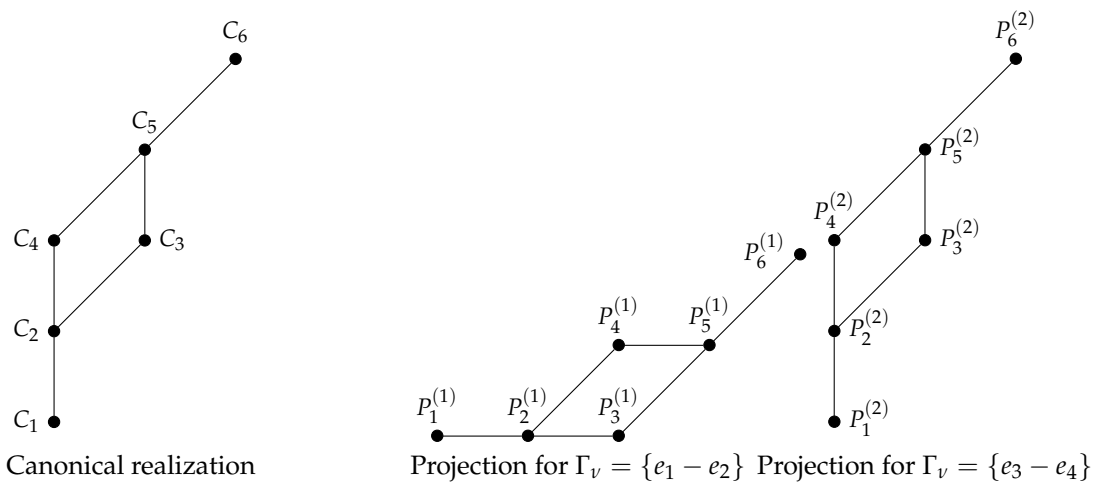


Figure 3.35: Example $\nu=EENN$.

Note that if we choose $\Gamma_\nu = \{e_3 - e_4\}$, we obtain the canonical realization up to translation.

Example 3.62

Consider the path $\nu = EENNEEN$ and use the labeling shown in Figure 3.36. By Lemma 3.52, the dimension of the maximal polytopal part is equal to $d = 3$. We choose exactly one element from $\{e_2 - e_3, e_4 - e_5\}$, let $\Gamma_\nu = \{e_2 - e_3\}$.

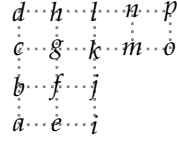


Figure 3.36: Grid for labeling of $\mathcal{SC}(Q_\nu, w_\nu)$ for $\nu = EENNEEN$.

Here is a list of all facets of the ν -subword complex $\mathcal{SC}(Q_\nu, w_\nu)$:

$$\begin{array}{llll} I_1 = \{a, b, c, d, e, i, m, o\} & I_2 = \{b, c, d, e, f, i, m, o\} & I_3 = \{b, c, d, f, i, j, m, o\} & I_4 = \{c, d, f, g, i, j, m, o\} \\ I_5 = \{c, d, g, i, j, k, m, o\} & I_6 = \{c, d, e, f, g, i, m, o\} & I_7 = \{d, e, f, g, h, i, m, o\} & I_8 = \{d, f, g, h, i, j, m, o\} \\ I_9 = \{d, g, h, i, j, k, m, o\} & I_{10} = \{d, h, i, j, k, l, m, o\} & I_{11} = \{d, h, i, j, l, m, n, o\} & I_{12} = \{d, h, i, j, l, n, o, p\} \\ I_{13} = \{a, b, d, e, i, m, n, o\} & I_{14} = \{b, d, e, f, i, m, n, o\} & I_{15} = \{b, d, f, i, j, m, n, o\} & I_{16} = \{b, d, f, i, j, n, o, p\} \\ I_{17} = \{d, f, h, i, j, n, o, p\} & I_{18} = \{d, e, f, h, i, m, n, o\} & I_{19} = \{a, b, d, e, i, n, o, p\} & I_{20} = \{b, d, e, f, i, n, o, p\} \\ I_{21} = \{d, f, h, i, j, m, n, o\} & I_{22} = \{d, e, f, h, i, n, o, p\} & & \end{array}$$

Here are the corresponding brick vectors after omitting the first and last coordinates:

$$\begin{array}{lll} b(I_1) = -(15, 11, 6, 9, 5)^\top & b(I_2) = -(15, 11, 5, 10, 5)^\top & b(I_3) = -(15, 11, 4, 10, 6)^\top \\ b(I_4) = -(15, 10, 4, 11, 6)^\top & b(I_5) = -(15, 9, 4, 11, 7)^\top & b(I_6) = -(15, 10, 5, 11, 5)^\top \\ b(I_7) = -(14, 10, 5, 12, 5)^\top & b(I_8) = -(14, 10, 4, 12, 6)^\top & b(I_9) = -(14, 9, 4, 12, 7)^\top \\ b(I_{10}) = -(13, 9, 4, 12, 8)^\top & b(I_{11}) = -(12, 10, 4, 12, 8)^\top & b(I_{12}) = -(11, 10, 5, 12, 8)^\top \\ b(I_{13}) = -(12, 14, 6, 9, 5)^\top & b(I_{14}) = -(12, 14, 5, 10, 5)^\top & b(I_{15}) = -(12, 14, 4, 10, 6)^\top \\ b(I_{16}) = -(11, 14, 5, 10, 6)^\top & b(I_{17}) = -(11, 12, 5, 12, 6)^\top & b(I_{18}) = -(12, 12, 5, 12, 5)^\top \\ b(I_{19}) = -(11, 14, 7, 9, 5)^\top & b(I_{20}) = -(11, 14, 6, 10, 5)^\top & b(I_{21}) = -(12, 12, 4, 12, 6)^\top \\ b(I_{22}) = -(11, 12, 6, 12, 5)^\top & & \end{array}$$

Here is a list of all projected points:

$$\begin{array}{llll} P_1 = -(15, 32, 41)^\top & P_2 = -(15, 31, 41)^\top & P_3 = -(15, 30, 40)^\top & P_4 = -(15, 29, 40)^\top \\ P_5 = -(15, 28, 39)^\top & P_6 = -(15, 30, 41)^\top & P_7 = -(14, 29, 41)^\top & P_8 = -(14, 28, 40)^\top \\ P_9 = -(14, 27, 39)^\top & P_{10} = -(13, 26, 38)^\top & P_{11} = -(12, 26, 38)^\top & P_{12} = -(11, 26, 38)^\top \\ P_{13} = -(12, 32, 41)^\top & P_{14} = -(12, 31, 41)^\top & P_{15} = -(12, 30, 40)^\top & P_{16} = -(11, 30, 40)^\top \\ P_{17} = -(11, 28, 40)^\top & P_{18} = -(12, 29, 41)^\top & P_{19} = -(11, 32, 41)^\top & P_{20} = -(11, 31, 41)^\top \\ P_{21} = -(12, 28, 40)^\top & P_{22} = -(11, 29, 41)^\top & & \end{array}$$

Below is a list of the points representing the canonical realization, illustrated in Figure 3.38.

$$\begin{array}{llll}
 C_1 = (0,0,0)^\top & C_2 = (0,0,1)^\top & C_3 = (0,0,2)^\top & C_4 = (0,1,3)^\top \\
 C_5 = (0,2,4)^\top & C_6 = (0,1,2)^\top & C_7 = (1,2,3)^\top & C_8 = (1,2,4)^\top \\
 C_9 = (1,3,5)^\top & C_{10} = (2,4,6)^\top & C_{11} = (3,4,6)^\top & C_{12} = (4,4,6)^\top \\
 C_{13} = (3,0,0)^\top & C_{14} = (3,0,1)^\top & C_{15} = (3,0,2)^\top & C_{16} = (4,0,2)^\top \\
 C_{17} = (4,2,4)^\top & C_{18} = (3,2,3)^\top & C_{19} = (4,0,0)^\top & C_{20} = (4,0,1)^\top \\
 C_{21} = (3,2,4)^\top & C_{22} = (4,2,3)^\top & &
 \end{array}$$

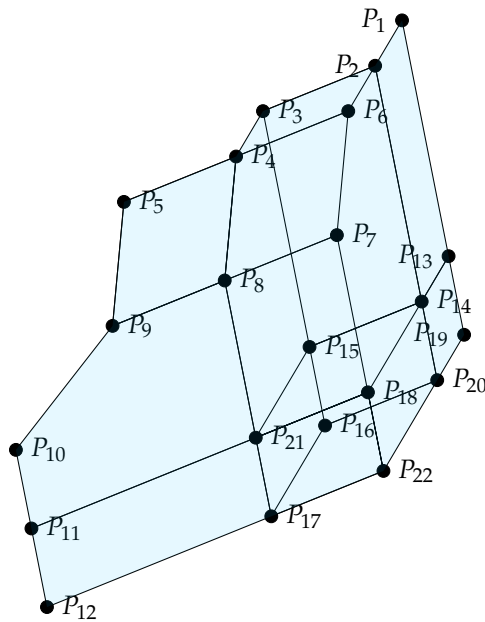


Figure 3.37: Projection of ν -associahedron for $\nu = EENNEEN$.

Remark 3.63

Note that the projected points differ from the canonical realization. However, I believe this idea can be used to further study ν -associahedra. We expect this approach to work in general, although it is not yet proven.

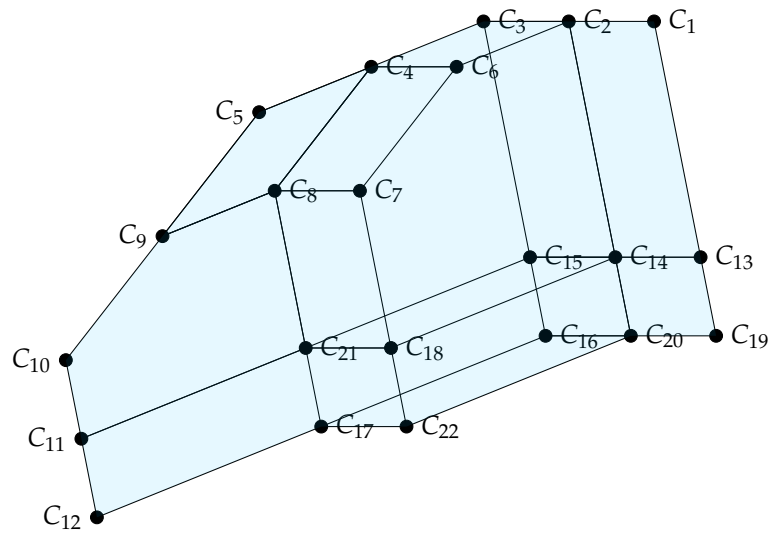


Figure 3.38: Canonical realization of ν -associahedron for $\nu = EENNEEN$.

Bibliography

Bibliography

- [Ber+23] Nantel Bergeron, Noemie Cartier, Cesar Ceballos, and Vincent Pilaud. *Lattices of acyclic pipe dreams*. 2023. URL: <https://arxiv.org/pdf/2303.11025>.
- [Ceb24] Cesar Ceballos. *A canonical realization of the alt ν -associahedron*. 2024. URL: <https://arxiv.org/abs/2401.17204v1>.
- [CLS14] Cesar Ceballos, Jean-Philippe Labbé, and Christian Stump. “Subword complexes, cluster complexes, and generalized multi-associahedra”. In: *J. Algebraic Combin.* 39.1 (2014), pp. 17–51. ISSN: 0925-9899,1572-9192. DOI: [10.1007/s10801-013-0437-x](https://doi.org/10.1007/s10801-013-0437-x). URL: <https://doi.org/10.1007/s10801-013-0437-x>.
- [CPS19] Cesar Ceballos, Arnau Padrol, and Camilo Sarmiento. “Geometry of ν -Tamari lattices in types A and B ”. In: *Trans. Amer. Math. Soc.* 371.4 (2019), pp. 2575–2622. ISSN: 0002-9947,1088-6850. DOI: [10.1090/tran/7405](https://doi.org/10.1090/tran/7405). URL: <https://doi.org/10.1090/tran/7405>.
- [CPS20] Cesar Ceballos, Arnau Padrol, and Camilo Sarmiento. “The ν -Tamari lattice via ν -trees, ν -bracket vectors, and subword complexes”. In: *Electron. J. Combin.* 27.1 (2020), Paper No. 1.14, 31. ISSN: 1077-8926. DOI: [10.37236/8000](https://doi.org/10.37236/8000). URL: <https://doi.org/10.37236/8000>.
- [CP20] Cesar Ceballos and Viviane Pons. “The s -weak order and s -permutahedra”. In: *Sém. Lothar. Combin.* 82B (2020), Art. 76, 12. ISSN: 1286-4889.
- [Ces22] Joseph Doolittle Cesar Ceballos. *Subword Complexes and Kalai’s Conjecture on Reconstruction of Spheres*. 2022. URL: <https://arxiv.org/pdf/2206.15461>.
- [Hoh12] Christophe Hohlweg. “Permutahedra and associahedra: generalized associahedra from the geometry of finite reflection groups”. In: *Associahedra, Tamari lattices and related structures*. Vol. 299. Progr. Math. Birkhäuser/Springer, Basel, 2012, pp. 129–159. ISBN: 978-3-0348-0404-2; 978-3-0348-0405-9. DOI: [10.1007/978-3-0348-0405-9_8](https://doi.org/10.1007/978-3-0348-0405-9_8). URL: https://doi.org/10.1007/978-3-0348-0405-9_8.
- [HL07] Christophe Hohlweg and Carsten E. M. C. Lange. “Realizations of the associahedron and cyclohedron”. In: *Discrete Comput. Geom.* 37.4 (2007), pp. 517–543. ISSN: 0179-5376,1432-0444. DOI: [10.1007/s00454-007-1319-6](https://doi.org/10.1007/s00454-007-1319-6). URL: <https://doi.org/10.1007/s00454-007-1319-6>.
- [Hum90] James E. Humphreys. *Reflection Groups and Coxeter Groups*. Cambridge University Press, 1990.
- [JS23] Dennis Jahn and Christian Stump. “Bruhat intervals, subword complexes and brick polyhedra for finite Coxeter groups”. In: *Math. Z.* 304.2 (2023), Paper No. 24, 32. ISSN: 0025-5874,1432-1823. DOI: [10.1007/s00209-023-03267-w](https://doi.org/10.1007/s00209-023-03267-w). URL: <https://doi.org/10.1007/s00209-023-03267-w>.

- [KM04] Allen Knutson and Ezra Miller. “Subword complexes in Coxeter groups”. In: *Adv. Math.* 184.1 (2004), pp. 161–176. ISSN: 0001-8708,1090-2082. DOI: [10.1016/S0001-8708\(03\)00142-7](https://doi.org/10.1016/S0001-8708(03)00142-7). URL: [https://doi.org/10.1016/S0001-8708\(03\)00142-7](https://doi.org/10.1016/S0001-8708(03)00142-7).
- [LL19] Dimitry Leites and Oleksandr Lozhechnyk. “Inverses of Cartan matrices of Lie algebras and Lie superalgebras”. In: *Linear Algebra Appl.* 583 (2019), pp. 195–256. ISSN: 0024-3795,1873-1856. DOI: [10.1016/j.laa.2019.08.026](https://doi.org/10.1016/j.laa.2019.08.026). URL: <https://doi.org/10.1016/j.laa.2019.08.026>.
- [PS12] Vincent Pilaud and Francisco Santos. “The brick polytope of a sorting network”. In: *European J. Combin.* 33.4 (2012), pp. 632–662. ISSN: 0195-6698,1095-9971. DOI: [10.1016/j.ejc.2011.12.003](https://doi.org/10.1016/j.ejc.2011.12.003). URL: <https://doi.org/10.1016/j.ejc.2011.12.003>.
- [PS15] Vincent Pilaud and Christian Stump. “Brick polytopes of spherical subword complexes and generalized associahedra”. In: *Adv. Math.* 276 (2015), pp. 1–61. ISSN: 0001-8708,1090-2082. DOI: [10.1016/j.aim.2015.02.012](https://doi.org/10.1016/j.aim.2015.02.012). URL: <https://doi.org/10.1016/j.aim.2015.02.012>.
- [Sch] Christoph Schulz. *Zitate über Mathematik*. URL: <https://www.careelite.de/en/galileo-galilei-quotes-sayings/> (visited on Apr. 10, 2023).